MET O 11 TECHNICAL NOTE NO 180

RAINFALL FORECASTS OVER CHINA

by

Wang Chao

Met O 11 (Forecasting Research Branch)
Meteorological Office
London Road
Bracknell
Berkshire
England.

December 1983

1. Introduction

The study and forecasting of occasions of severe weather is one of the major tasks of Chinese meteorologists. The forecasting of rainstorms is of particular importance since these features are quite common and often lead to flash floods bringing much damage and human suffering. Summer is the rainy season in China when the prevailing southwesterly monsoon winds bring warm moist unstable air from the Indian Ocean and the South China Sea. Consequently there is considerable convective activity and heavy showers and thunderstorms contribute largely to the total summer rainfall. More organised areas of heavy convective rainfall may occur along the convergence zone that forms ahead of these moist southwesterlies. A strong low level jet is often associated with the most vigorous of these rainstorms acting as a source of both moisture convergence and instability [Sun (1983)].

Tropical cyclones and typhoons are also a constant danger in coastal regions during the summer months although these are usually short lived. Severe weather can also occur in Spring as warmer air moves northwards. The Yellow River basin is a favoured area for the formation of intense cyclones at this time of the year and these often give rise to heavy rainfall. The maximum amount of precipitation observed in some of the provinces of China gives an indication of the intensity of these features; 198.7mm in one hour in Hanam, 664mm in 12 hours in Guangdang, 950mm in 24 hours in Hebei and 1672mm in 24 hours in Taiwan [Zhang

(1979)].

Over the years Chinese weather forecasters have developed a set of empirical forecasting tools based on synoptic theory and their forecasting experience. Tao (1979), for example, quotes the "weather form" method, in which the distributional characteristics of various types of weather systems both at the time of the occurence of rainstorms and before it are used as predictors, and also the "area of fall" or "drop" method for forecasting rainfall locations which depends on the various physical conditions which exist when rainstorms occur. By using these and other methods the forecasters can usually tell when and where rainfall will occur and also the approximate amount. Nevertheless, large precipitation events are not easily forecast even by the most senior of forecasters. It is, of course, just such events that we are most anxious to predict.

The use and development of numerical weather forecasting models is still in its early stages in China. A four level hemispheric primitive equation model with a horizontal gridlength of 380km is run once a day at the Beijing Centre of Meteorology, providing forecasts for up to three days ahead, whilst in Shanghai and Guangzhon numerical models are used for typhoon forecasting and research into tropical meteorology [W.M.O. (1983)]. It is hoped that the further development of these models will eventually lead to good objective forecasts of areas of very heavy precipitation. High resolution versions will undoubtedly be necessary in order to resolve the localised nature of such features. These will take the form of regional models because of the constraints imposed by the speed and size of present day computers. To this end much work has been done towards developing an IBM Fortran version of the Meteorological Office's operational limited area model, so that this may be used in China to promote further study of these features. See Appendix A.

The Meteorological Office makes global forecasts twice a day from 00z and 12z data using a 15 level model with a latitude-longitude grid of $1.5^{\circ} \times 1.875^{\circ}$. Because of its global coverage this model may be used to assess the current quality of numerical precipitation forecasts over China, although it should be noted that the model's horizontal resolution of 150 km may not be fine enough to resolve all the important small scale features. Also it is very likely that the parametrization of the convective precipitation processes [Lyne and Rowntree (1976)] used by the forecast model will be unable to represent the local effects of the large convective storms that generally give rise to rainstorms, since the scheme is designed to represent the average effect of many convective plumes within a gridbox. Nevertheless, an examination of the precipitation forecasts produced by this model is still of interest and may indicate some of the advantages and disadvantages of its current formulation. An assessment of the global model's performance in forecasting the weather over China is also of interest to the Meteorological Office since the operational forecasts are not normally examined over this region.

Two cases are presented in the following pages which are thought to be representative of some of the synoptic developments that lead to severe rainstorms. 48 hour forecasts are used to examine both rainfall accumulations and the ability of the model to reproduce the important synoptic features.

2. Case 1 : A Yellow River cyclone. (Data time 00z 24/4/83.)

This is an example of a midlatitude cyclone which forms in the Yellow River basin and produces large amounts of rainfall as it moves away northeastwards.

2.1 The synoptic situation

In Spring cold continental air which covers the north of China during the winter begins to recede northwards being replaced by warmer air from the south. An area of strong thermal contrast exists between these two air masses during this transitional period and it is thus a favoured time for the formation of intense cyclones. Also the Yellow River basin is situated downstream of the huge highland masses of Tibet and Qinghai making this a prefered area for cyclogenesis.

Only 12z verifying charts are available from the daily weather reports issued by the Japanese Weather Agency. These correspond to 12 hours and 36 hours into the forecast. Figures 1a and 1b show the 500 mb development. A marked troughing of the 500 mb flow is apparent where the jet splits over central China and merges again along the eastern Pacific coastline. This trough sharpens and intensifies as warm moist air is channelled along its forward side by the strong southwesterly flow around the subtropical anticyclone over the South China Sea. At 850 mb (Figures 2a and 2b) a cyclone forms over the lower reaches of the Yellow River a little ahead of a strong thermal trough. This moves northeastwards during the period 12z 24/4/83 to 00z 25/4/83.

The 850 mb fields of dew point depression show a moist tongue extending northwards over eastern China. (See Figure 3). This tongue becomes narrower and moister as the upper trough moves eastwards and the ridge of the subtropical high becomes more intense. This is the source of the heavy precipitaion that occurs between 12z 24/4/83 and 00z 26/4/83.(See Figures 5b, 5c and 5d). A great quantity of moisture is transported by the southwesterly flow which increases in speed during this period. This can be seen from Figures 4a and 4b which show isotachs of the 850 mb winds. There is also a large increase in wind shear as the system develops. This corresponds to an area of increasing horizontal convergence and ascending motion. The centre of the rainfall area is nicely consistent with this shear line.

2.2 The forecast

a. *Precipitation*

Generally speaking the rainfall forecasts from the global model are very satisfactory and it is felt that they would be quite useful to forecasters. There are faults, however, these being mostly because the forecast rainfall areas are too widespread.

The beginnings of the rainfall associated with this cyclone can be seen from Figure 5a, the observed 12 hour accumulation of precipitation for the period 00z - 12z on 24/4/83, where a maximum of 4mm is shown around the eastern part of Gansu province (105°E, 35°N). Over the next 24 hours this rainfall area grows so much that it covers most of eastern China, a maximum of 40mm being observed in the period 00z - 12z on 25/4/83. As the cyclone moves northeastwards in the final period most of the heavy precipitation falls over NE China, but a heavy rainfall centre still remains over the lower reaches of the Yellow River. (See Figure 5d).

Let us now examine the precipitation forecasts produced by the global model. Over the 48 hours of the forecast the rainfall area moves northeastwards as observed. The distribution and maxima of the forecast precipitation areas are also in general agreement with the observations. For example, in the period 00z - 12z on 25/4/83 the maximum is 40mm in both Figure 5c, the observed accumulations, and Figure 6c, the forecast accumulations. In the final 12 hours of the forecast the two observed maxima are 28mm and 42mm located in Sandong (117°E, 37°N) and Liaoning (129°E, 40° N) provinces. The global model gave two centres with maxima of 17mm and 28mm. The positions of the forecast centres are within

200 km of their observed positions. (See Figures 5d and 6d). Consequently the maintenance of the rainfall over the lower reaches of the Yellow River was handled extremely well.

Now let us look at some of the errors in the precipitation forecast. Widespread areas of between 0 and 5 mm are quite common around the edges of the main rainfall regions most of which are not confirmed by the observations. But dry stable areas are correctly forecast; note the dry regions associated with the subtropical Pacific anticyclone and the diffluent flow over the Sea of Japan. The most serious error is in the period 00z - 12z on 25/4/83 where an erroneous rainfall area with a maximum of more than 30mm is produced by the model near the mouth of the Yangtze River. A similar mistake also occurs in the northeastern part of the country, where a spurious centre of 25mm is produced.

b. *The associated synoptic systems*

Figures 7 and 8 are the 12 hour and 36 hour forecasts that compare with Figures 1 and 2 the analysed 500 mb and 850 mb height fields. The subtropical high pressure area is handled very well by the forecast, although its intensity is underdone in the early stages. (Compare the 588 decameter contours in Figures 7a and 1a). The upper trough is well positioned throughout the forecast but it is not as sharp nor does it extend as far south as in the analysis. At 850 mb the cyclone is well developed by the model forming a strong gradient in the southwesterly flow at 36 hours. This is confirmed by the forecast wind fields (Figures 9a and 9b) where the formation of the belt of very strong winds ahead of the thermal trough is very well represented. The jet maximum of 60kts is also verified by the observations.

There are some inconsistencies between the forecast and observed wind fields particularly in the western part of China. This is because the wind charts are output on sigma levels and these cannot be compared with pressure level charts over high topography.

Finally, let us examine the relative humidity forecasts. The 36 hour chart shows the moist tongue extending from the mouth of the Yangtze River to the northern part of China. In fact this is not as far as in the observational chart (Figure 3). Thus some of the errors in the rainfall forecasts mentioned above could be partly caused by this error in the humidity field.

2.3 Conclusions

The main characteristics of the generation of the Yellow River cyclone were reproduced successfully by the U.K. operational global model. In particular it handled the extension of the subtropical anticyclone and the formation of the strong wind shear in the southwesterly flow very well. The rainfall forecasts were reasonable and the motion of the area of heavy rainfall was correctly predicted.

The spatial extent of the forecast rainfall was in general too large. This may be due in part to the coarseness of the horizontal gridlength, but is most likely a consequence of a known deficiency in the parametrization of the operational deep convection scheme. The current formulation of this scheme allows the production of precipitation whenever cloud forms. Thus, for example, precipitation may fall from shallow cumulus. Proposed modifications, as yet to be tested, will inhibit precipitation until a critical cloud depth has been reached.

3. Case 2 : An example of a low-level jet. (Data time 00z 28/7/88.)

This is an example of a summer monsoon case where some of the small scale features often associated with rainstorms, notably a low level jet and shallow low-level vortices, are observed.

3.1 The synoptic situation.

The synoptic situation is illustrated by Figure 11a, a chart of the 850mb streamlines at 00z 29/7/83 provided by the Beijing Centre of Meteorology. This situation persisted for several days bringing large amounts of precipitation. (See Figures 12a - 12b). During this period several shallow small scale depressions formed and moved along the shear line that exists between the moist southwesterly flow and the continental air mass.

The exact timing of the position and intensity of these shallow vortices may be important for a good numerical prediction of the rainfall centres, but many only have horizontal dimensions of around 300 km, not much greater than a model gridlength.

3.2 The forecast

a. *The 850mb winds*

Figure 11b is the 24 hour forecast wind field that corresponds to Figure 11a, the 850mb streamline analysis chart. The area of strong southwesterly winds over eastern China is well modelled at this stage of the forecast, with the maximum wind speed of 45 kts being confirmed by the observations. Notice also that two areas of cyclonic circulation are present along the northern edge of the convergence zone, suggesting that the forecast is able to model these features. Although, in this case, their number and positions do not correspond with those in the analysis chart.

b. *Precipitation*

From Figures 12a - 12b, the four charts of observed accumulated precipitation, it is clear that the precipitation occurs along a narrow zone stretching in a southwesterly direction from the mouth of the Yellow River. Indeed the lower and middle reaches of the Yangtze River are completely dry throughout this period. Localised areas of very heavy rainfall are observed within this rainfall zone, many being greater than 30mm in a 12 hour period.

The corresponding forecast charts (Figures 13a -13b) show general agreement with the observations in the positioning of the zone of heavy precipitation, but the errors in the prediction of the individual rainfall centres are quite considerable. The criticism, stated in Section 2, of the forecast rainfall areas being too widespread may also be applied here, although the forecast periods which include most of the Chinese night (Figures 13b and 13d) are much better at predicting the dry conditions along the Yangtze River basin.

The local maximas of rainfall predicted by the forecast are much fewer than observed and their amounts are generally underforecast, particularly at night.

c. *The low-level jet*

Figures 14a - 14c are the observed wind speeds for 12z on 29/7/83 for 500, 700 and 850 mb. These show a maximum at 700mb, indicating that the strongest winds are below 500mb.

Figures 15a -15c are the 36 hour fields that correspond to the above. These show the strongest wind speeds to be at sigma level 4 (870mb). Thus the model has produced a low-level jet, although it is more extensive and at a lower level than the observed feature.

3.3 Conclusions

This forecast indicates that the model is capable of representing both the low-level jet and the shallow vortices which are often associated with rainstorms. The model was unable to predict these features with enough accuracy, however, to give a detailed picture of the associated precipitation areas. Forecasts with a higher horizontal resolution may be more successful.

The rainfall produced by the global model shows a strong diurnal variation, indicating that much of it is forced by solar heating. On the other hand, the observed precipitation does not exhibit this characteristic, with the large outbreaks of precipitation persisting throughout the night.

4. Acknowledgements

I wish to express my sincere thanks to Dr A. Dickinson for his guidance throughout the course of this work. I am also grateful to other members of the Forecasting Research Branch for their valuable help.

References

Dickinson A. and Dutton M. — Limited area modelling in the UK Meteorological Office. L.A.M. Newsletter No 4, 1981

Lyne W.H. and P.R. Rowntree — Development of a convective parametrization using GATE data. Met O 20 Tech Note II/70, 1976

Sun S. — The effects of the low level jet on the stability of gravity waves. Scientia Atmospherica Sinica, Vol 7, No 2, June 1983.

Tao S-Y — Research on storm and strong convection weather. Scientia Atmospherica Sinica, Vol 3, No 3, Sept 1979.

W.M.O. — Meteorology in China today. W.M.O. Bulletin, Vol No 2, April 1983.

Yeh T-C — The recent advances in research into atmospheric science in China. Scientia Atmospherica Sinica, Vol 3, No 3, Sept 1979.

Zhang Y — Advances in heavy rain forecasting research in China. Meteorological Monthly, No 11, Nov 1979.

Appendix A

A standard Fortran version of the UK operational fine mesh model has been derived so that this model may be run on the Hitache M170 computer at the Beijing Centre of Meteorology. Since this computer is much slower (1 mip) than those used in Bracknell it has been necessary to reduce the area and increase the horizontal gridlength in order to reduce the computer time taken to an acceptable level.

The test areas that are currently being used are shown in Figure 16. Integrations over the larger area are done with a resolution of $1.5^{\circ} \times 1.875^{\circ}$, the same as is used by the UK global model. The inner area uses a finer resolution of $0.75^{\circ} \times 0.9375^{\circ}$. This has allowed the testing of routines to generate boundary values for the inner area from a forecast over the larger area.

One advantage from this choice of areas is that the Fourier chopping method [Dickinson and Dutton (1981)] necessary at high latitudes in order to maintain stability is not required, thus giving a considerable saving in computer time.

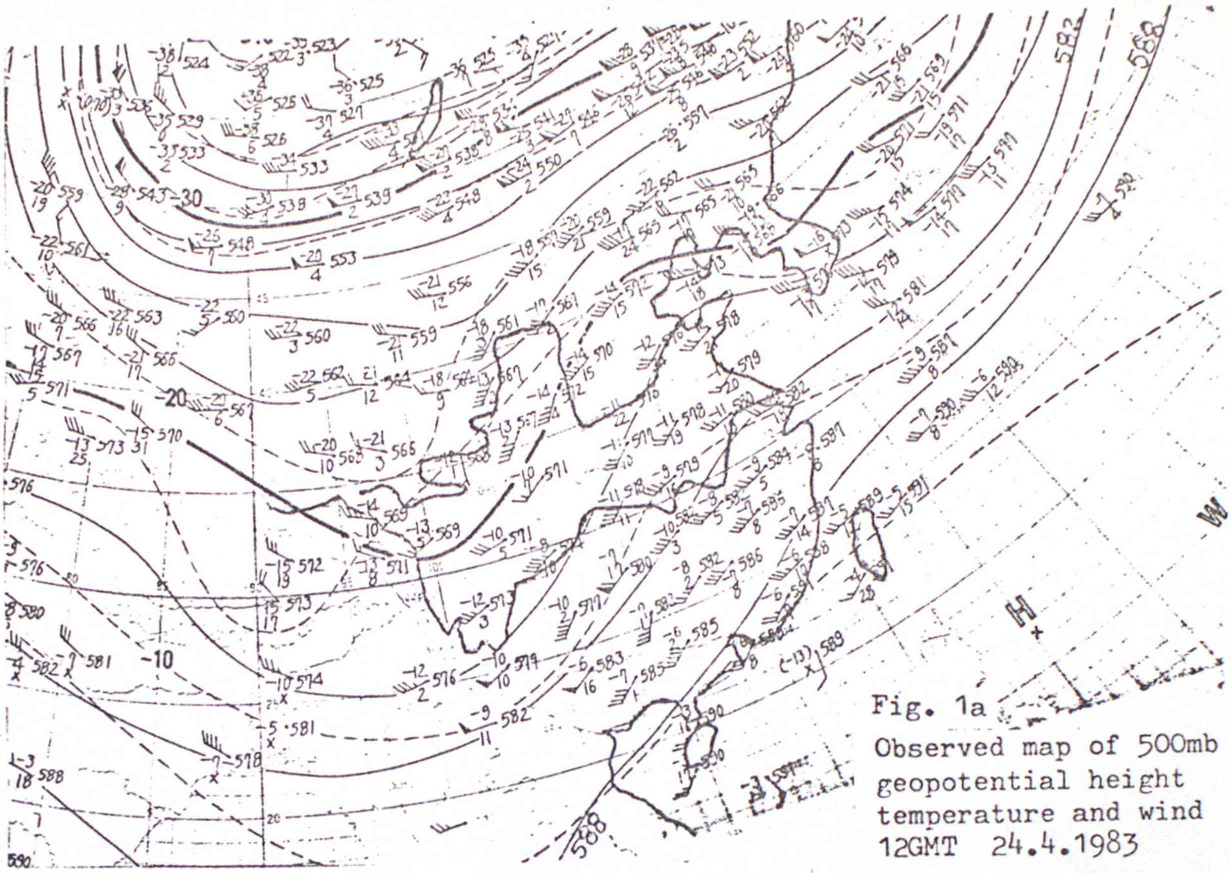

Fig. 1a
Observed map of 500mb geopotential height temperature and wind 12GMT 24.4.1983

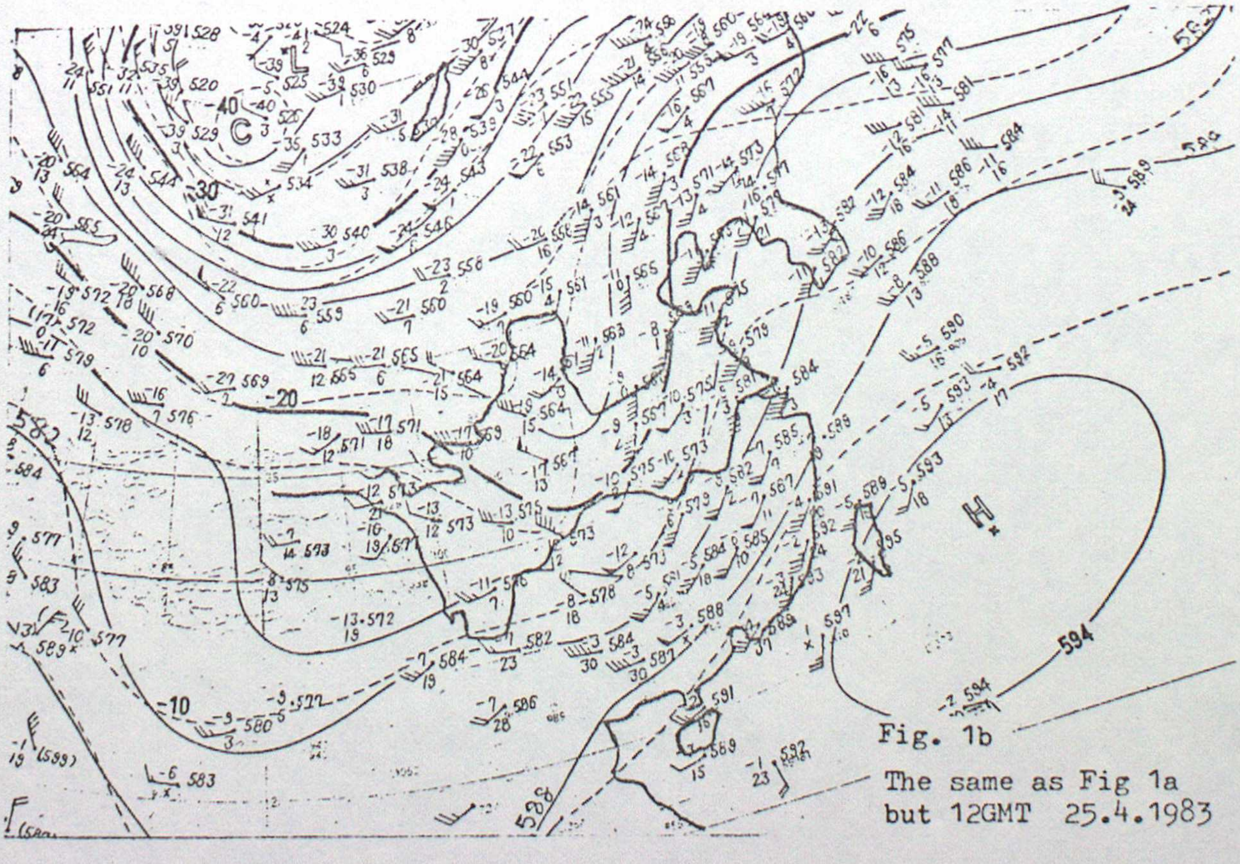

Fig. 1b
The same as Fig 1a but 12GMT 25.4.1983

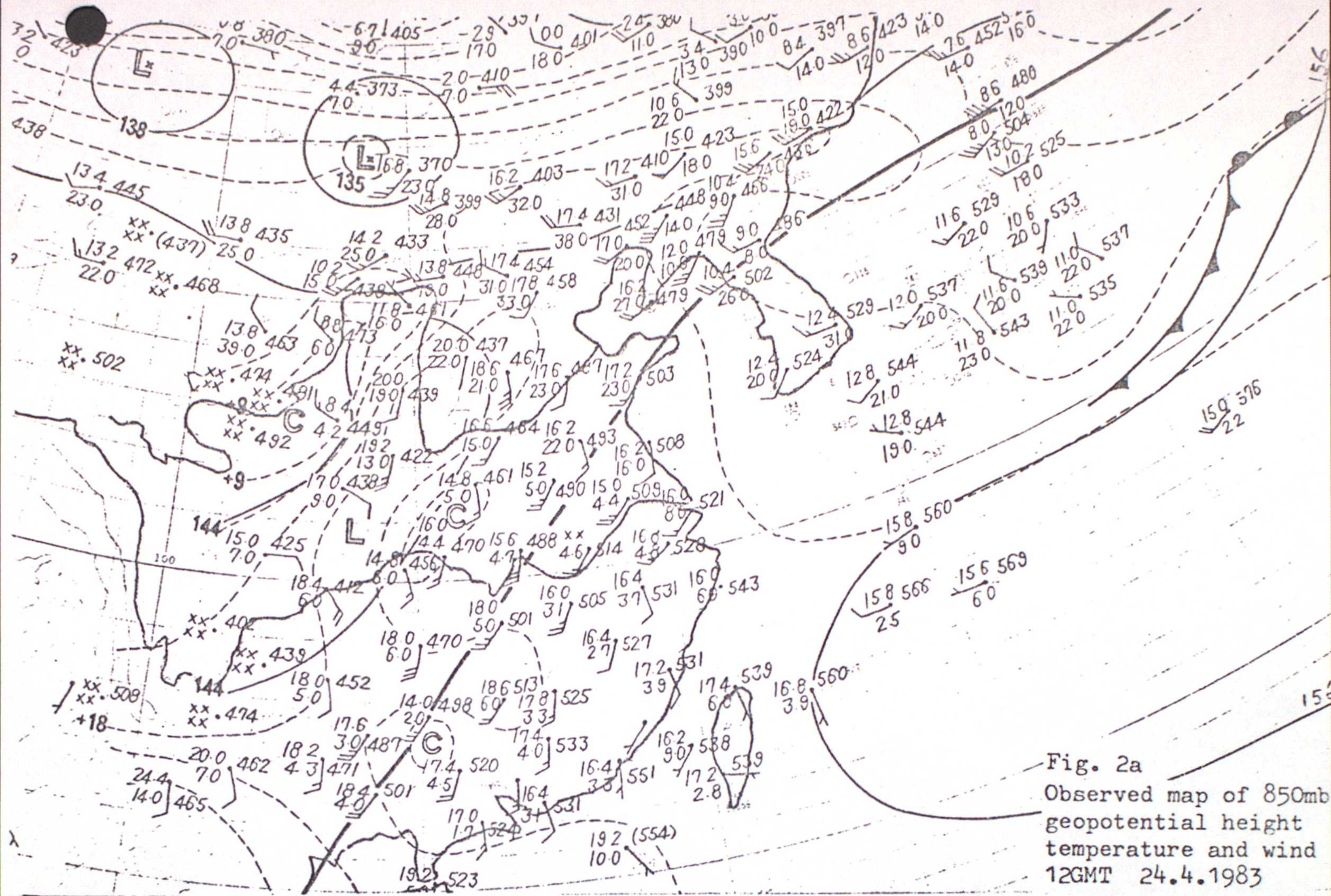

Fig. 2a

Observed map of 850mb geopotential height temperature and wind 12GMT 24.4.1983

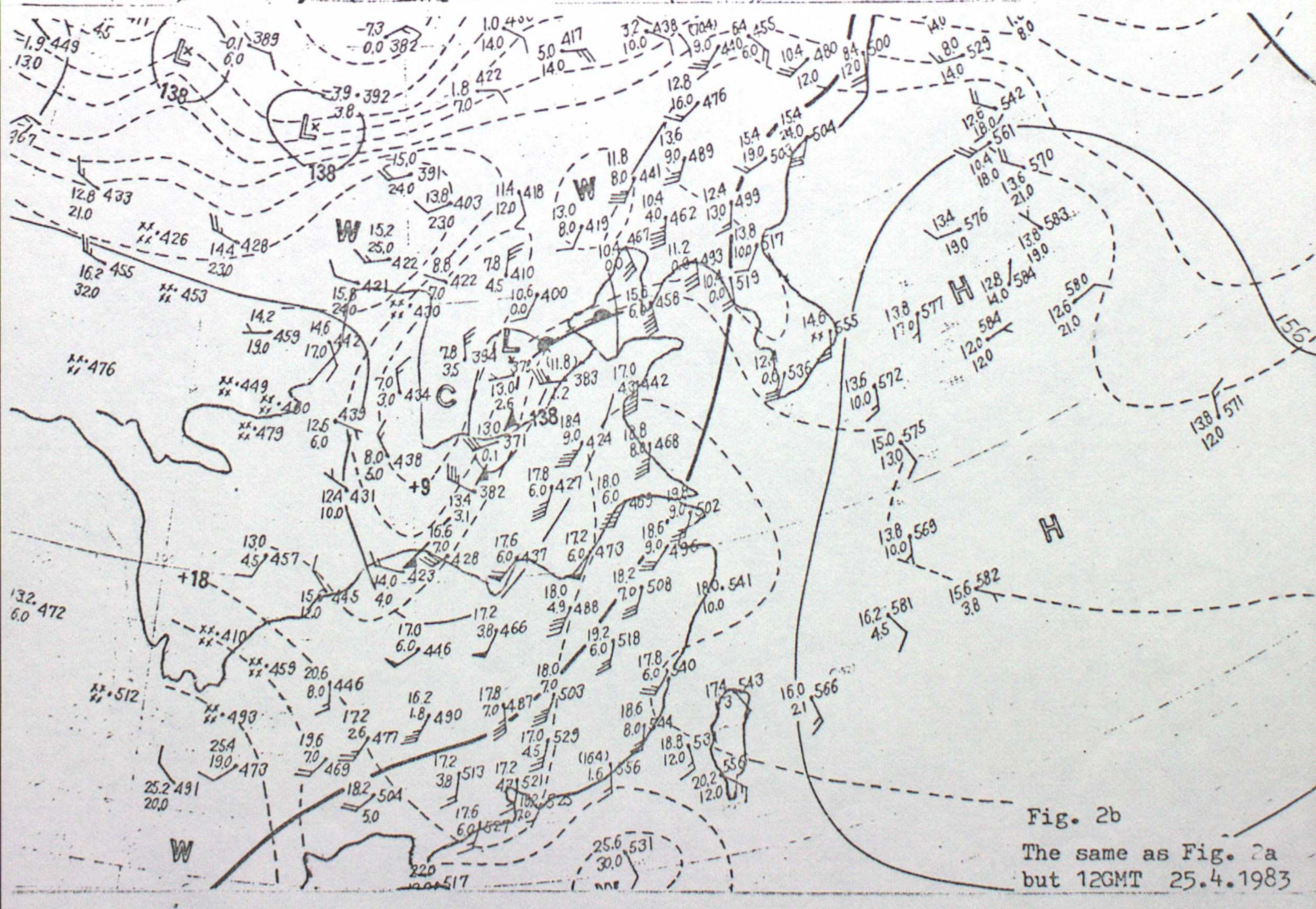

Fig. 2b

The same as Fig. 2a but 12GMT 25.4.1983

Fig. 3 Observed T-Td (^{o}C) 850mb
12GMT 24.4.1983

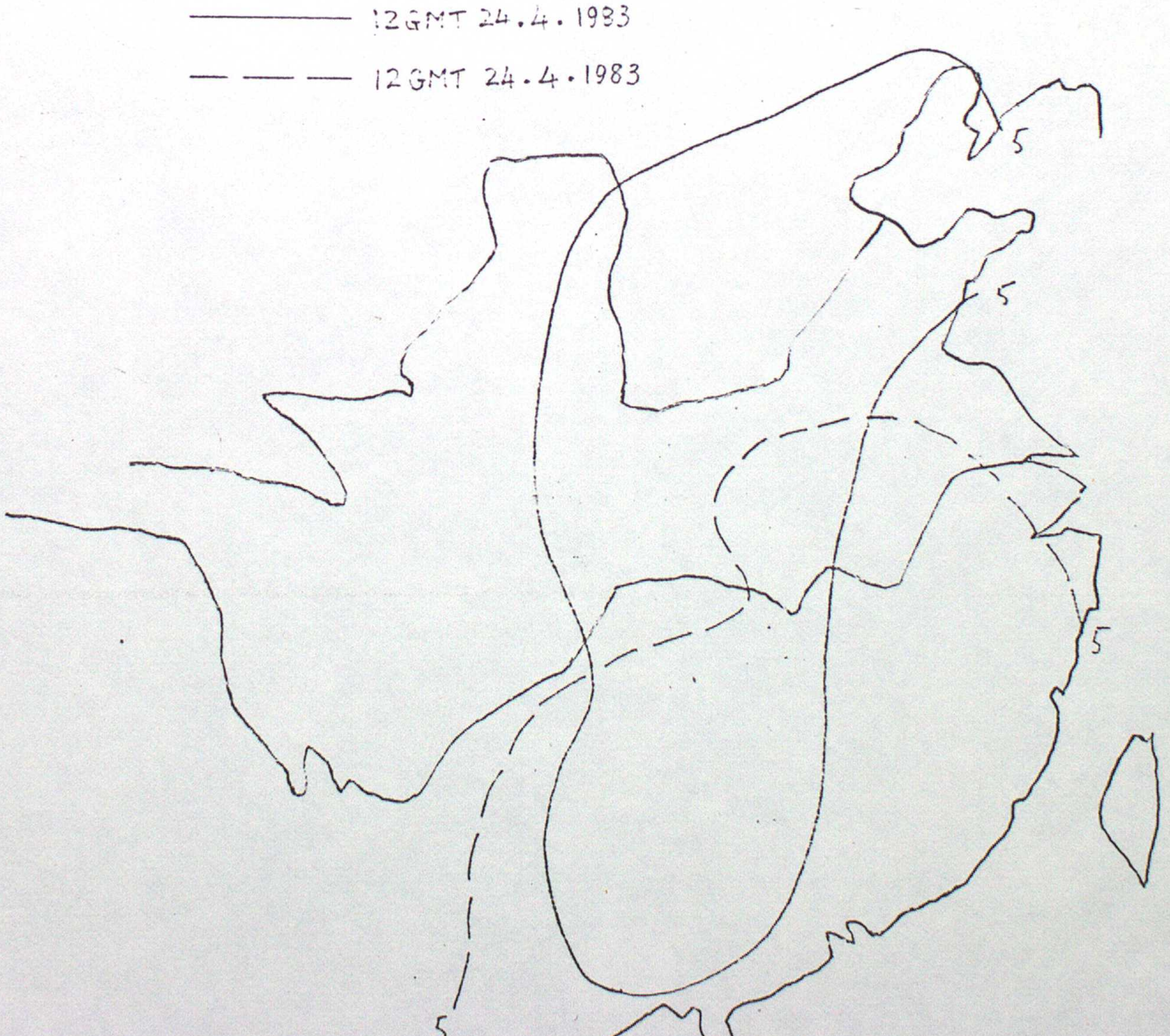

Fig. 4a Isotach (M/S) 850mb
12GMT 24.4.1983

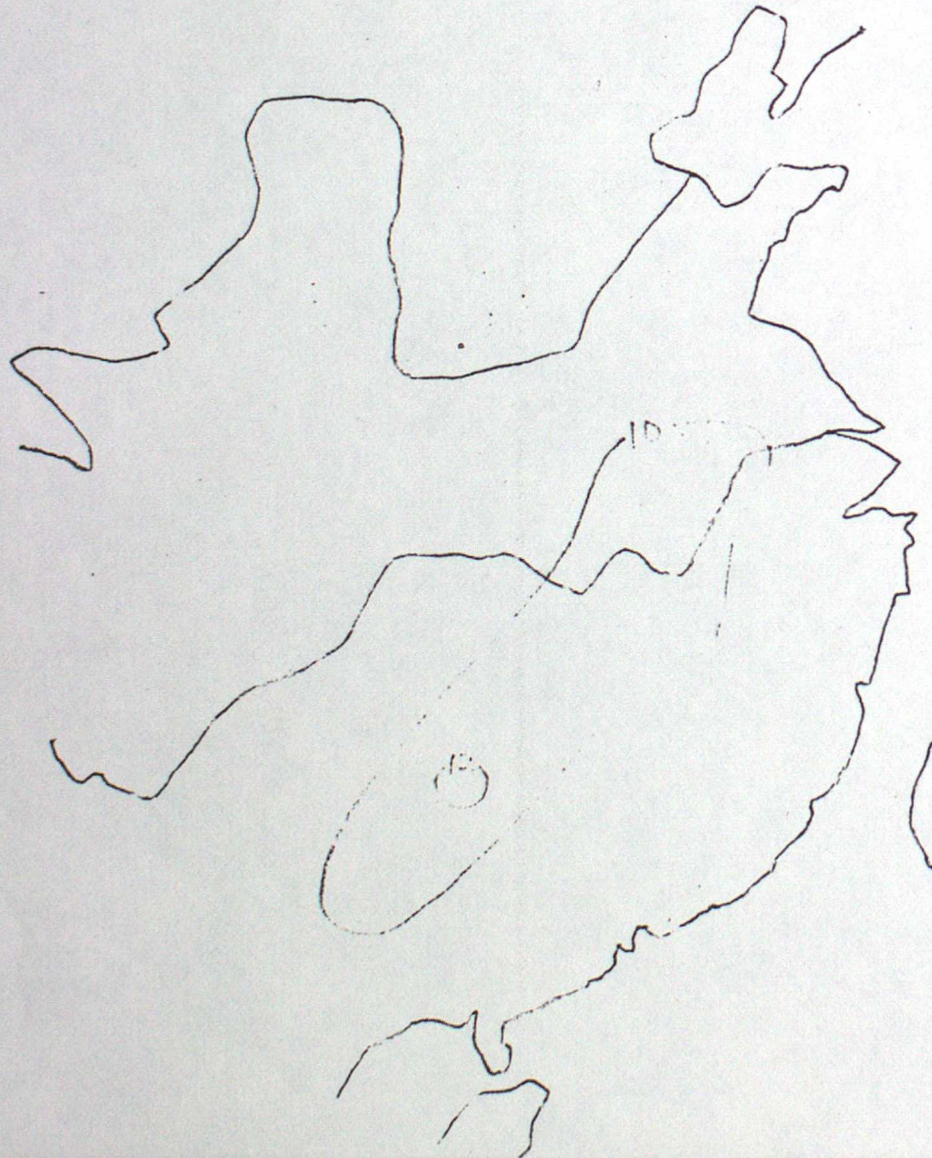

Fig. 4b The same as Fig. 4a
but 12GMT 25.4.1983

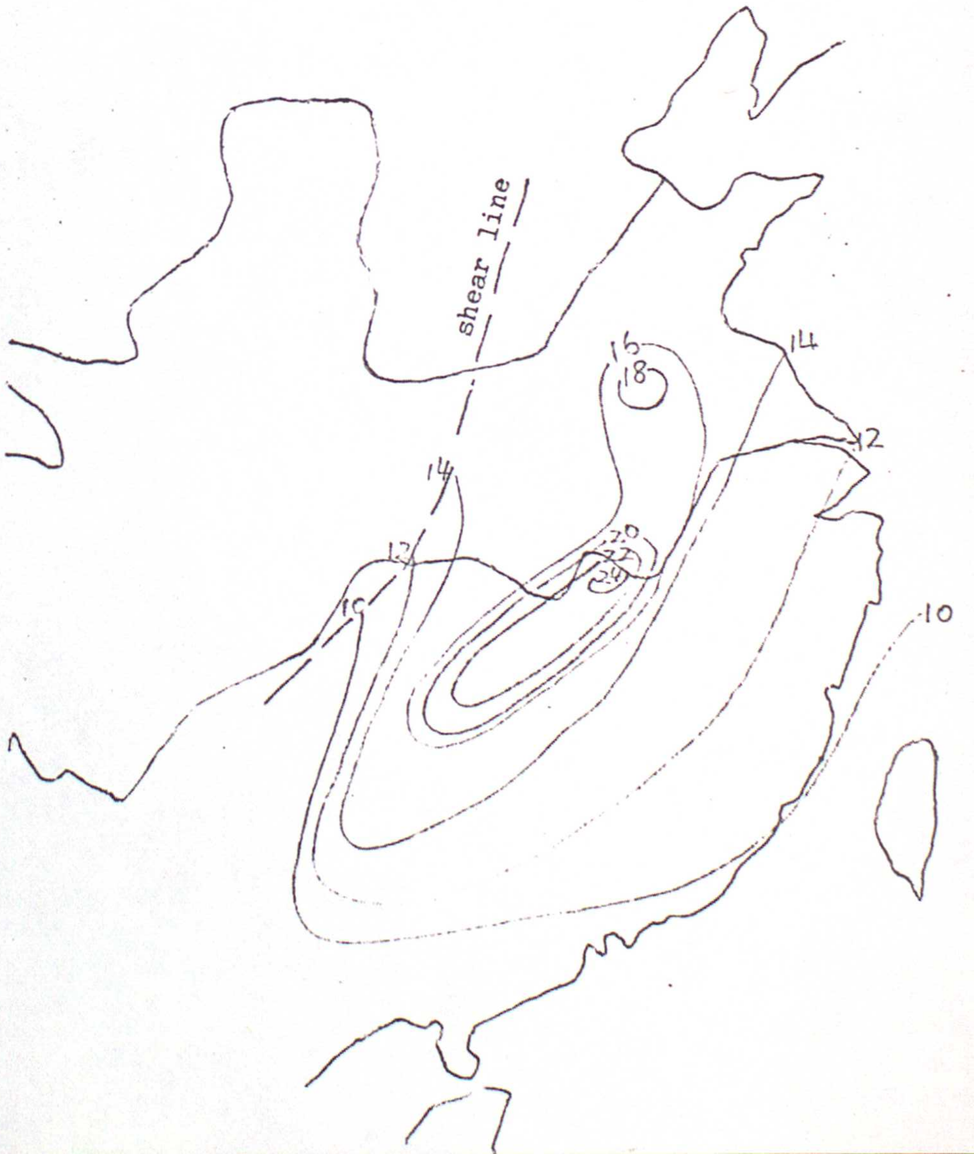

Fig. 5a RAINFALL(MM) 0000/24/04/83 TO 1200/24/04/83

Fig. 5b RAINFALL(MM) 1200/24/04/83 TO 0000/25/04/83

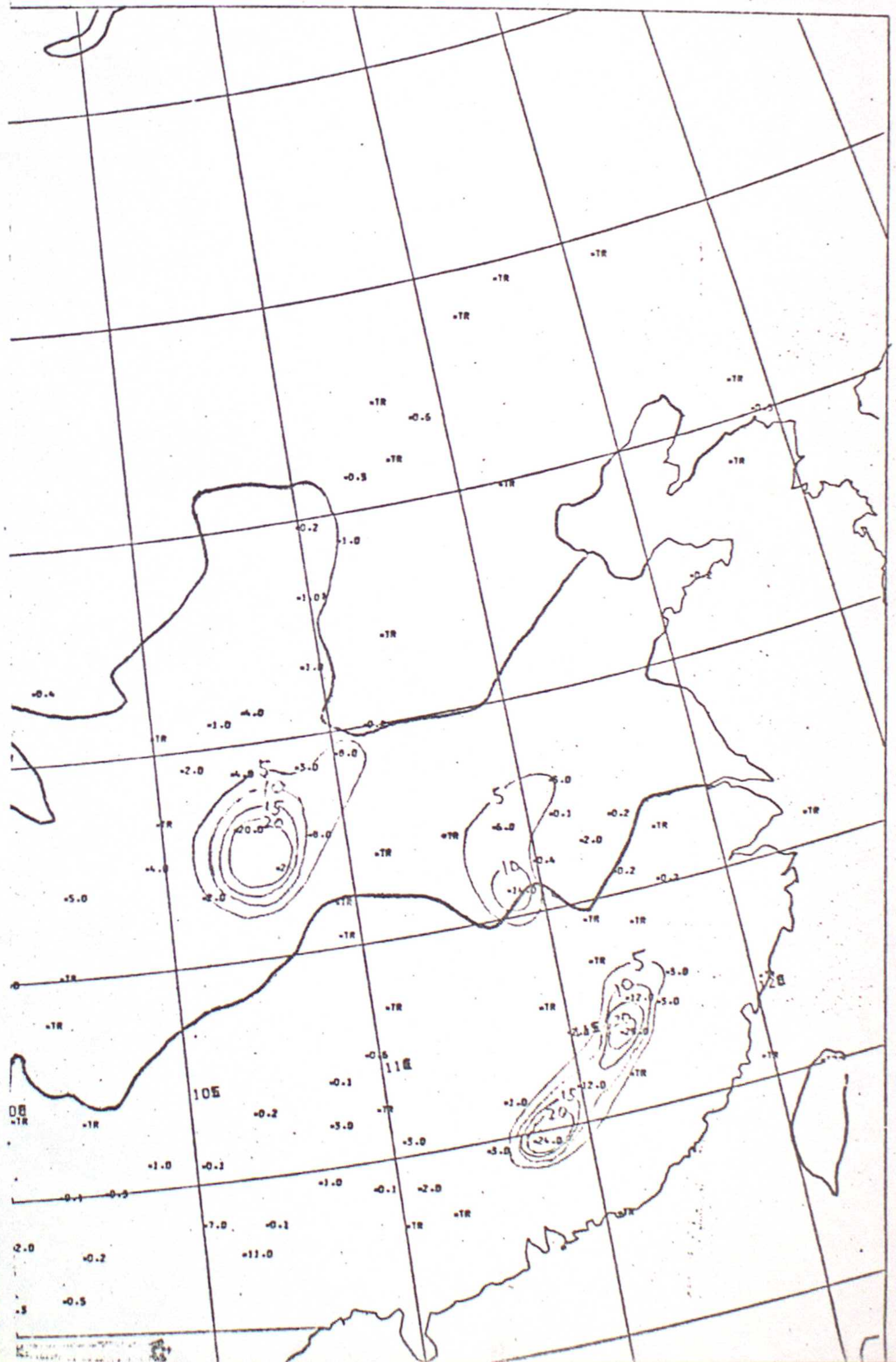

Fig. 5c RAINFALL(MM) 0000/25/04/83 TO 1200/25/04/83

Fig. 5d RAINFALL(MM) 1200/25/04/83 TO 0000/26/04/83

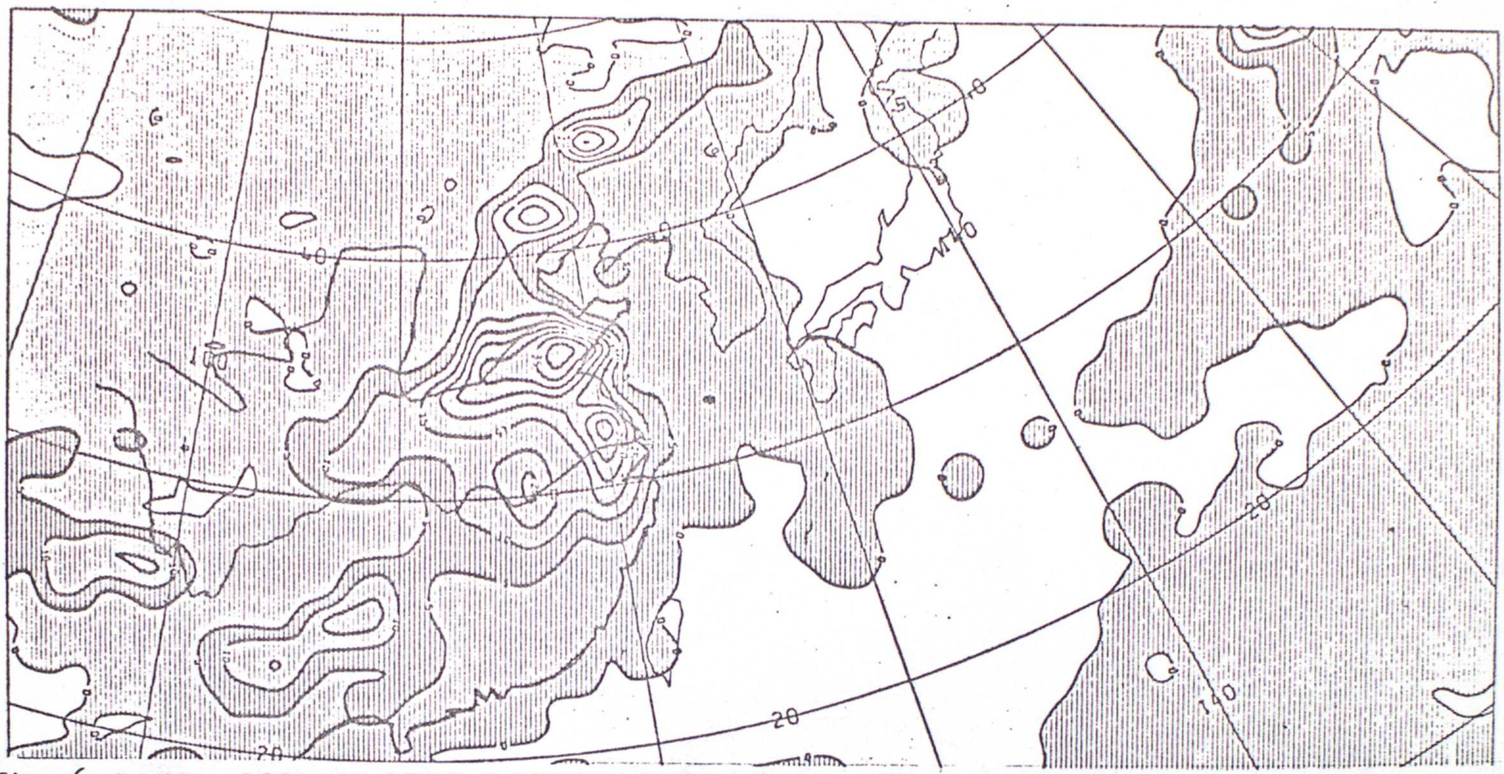

Fig. 6c TOTAL ACCUMULATED PRECIPITATION MM DT 0Z 24/4/1983
VT 12Z 25/4/1983

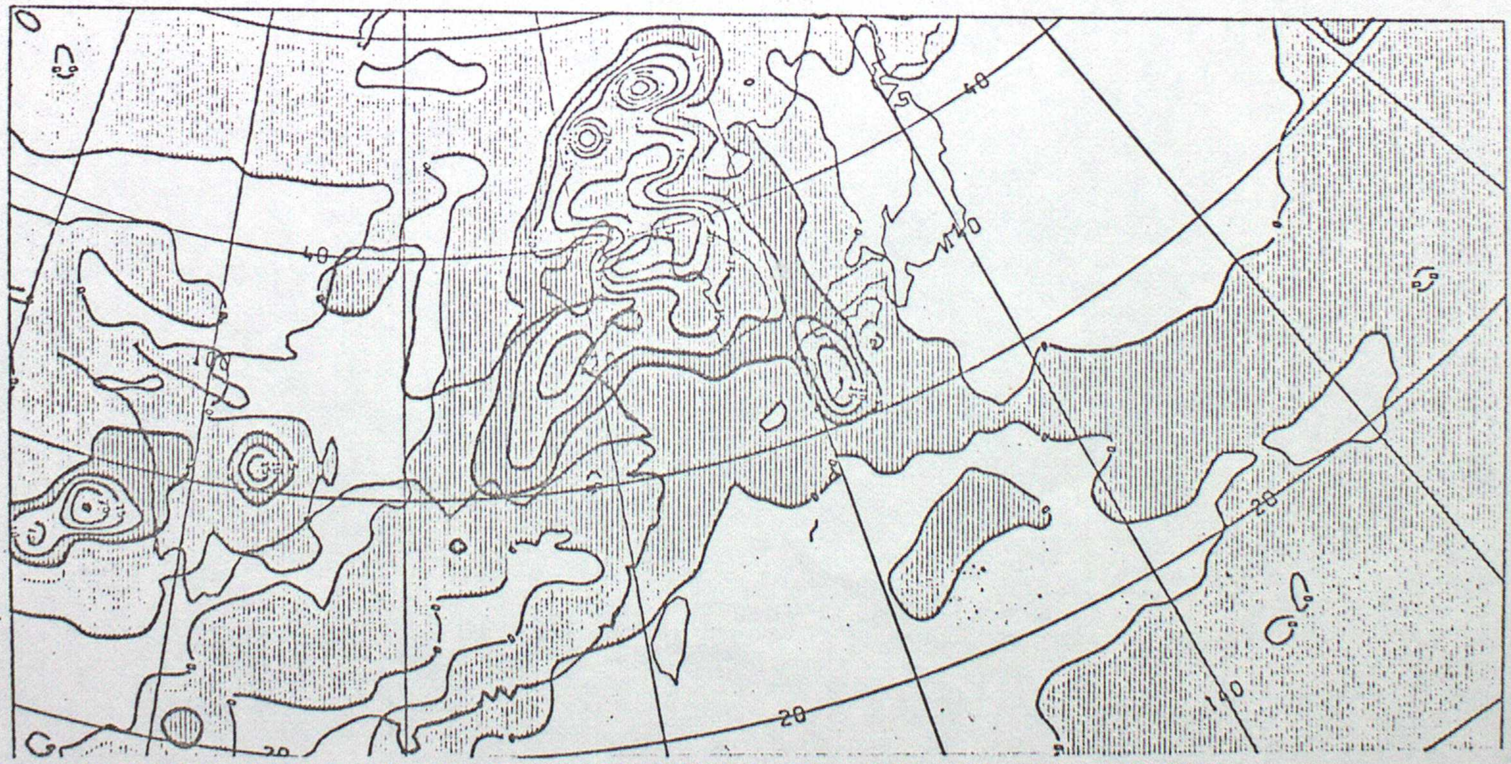

Fig. 6d TOTAL ACCUMULATED PRECIPITATION MM DT 0Z 24/4/1983
VT 0Z 26/4/1983

Fig. 6a TOTAL ACCUMULATED PRECIPITATION MM DT 0Z 24/4/1983
VT 12Z 24/4/1983

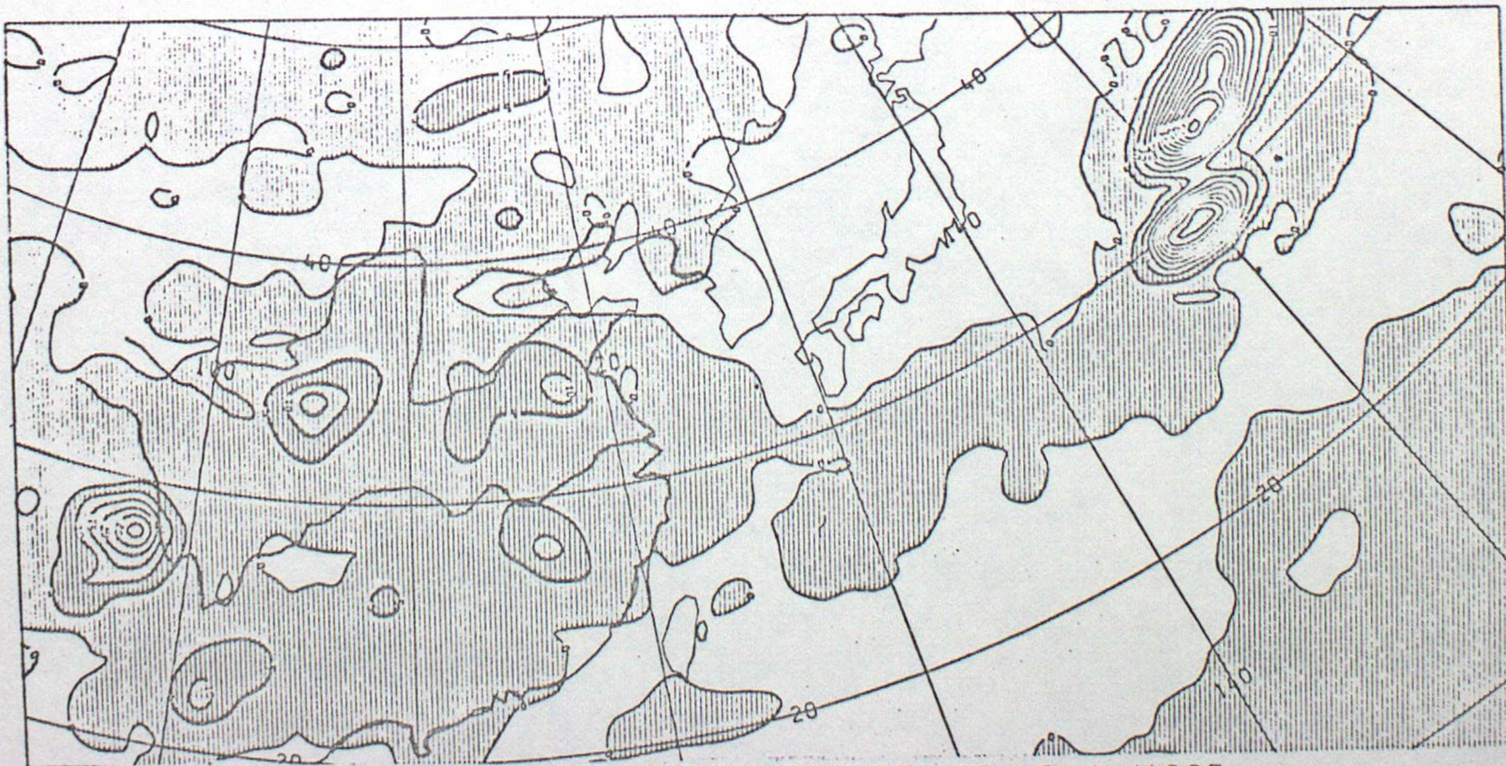

Fig. 6b TOTAL ACCUMULATED PRECIPITATION MM DT 0Z 24/4/1983
VT 0Z 25/4/1983

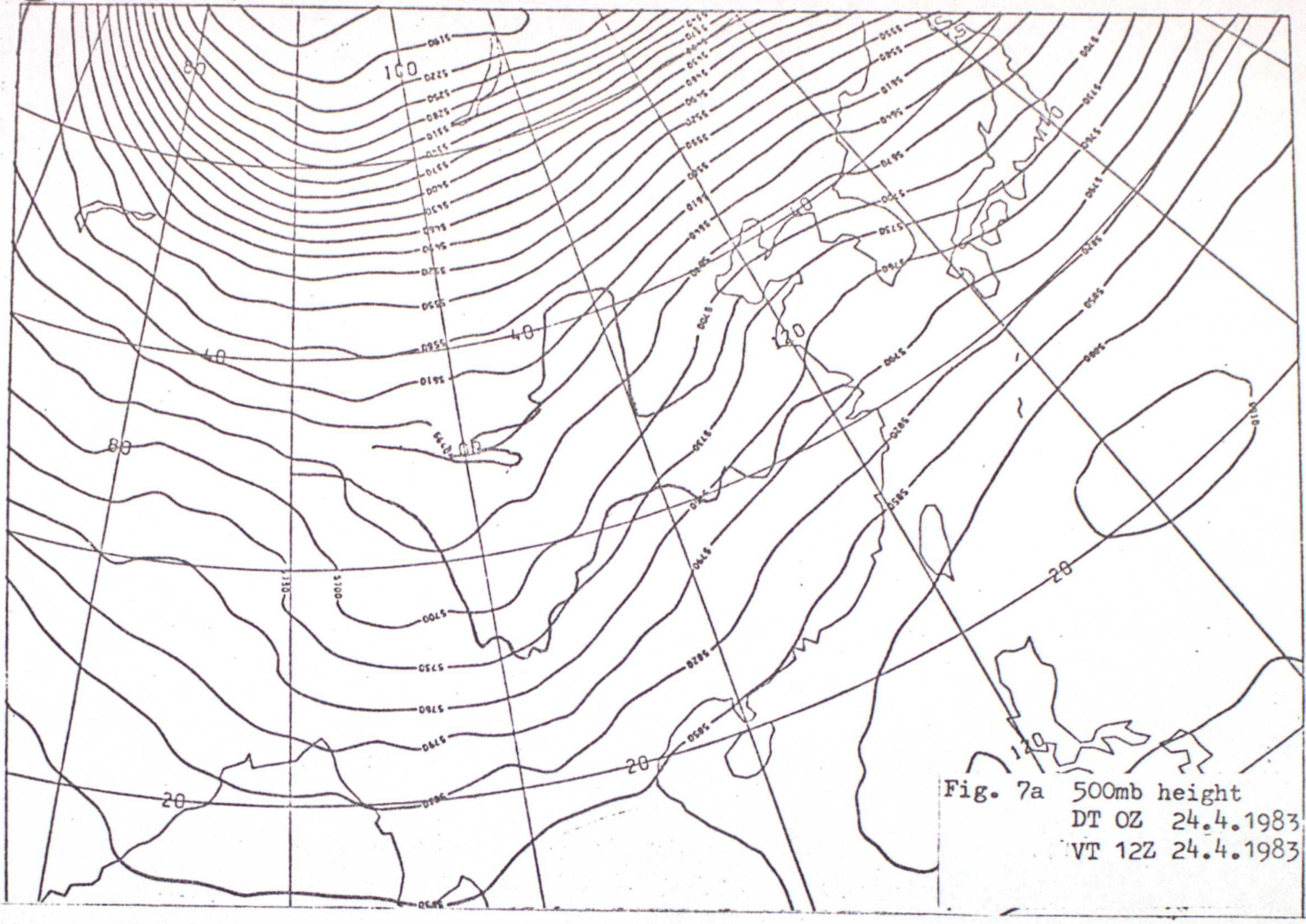

Fig. 7a 500mb height
DT 0Z 24.4.1983
VT 12Z 24.4.1983

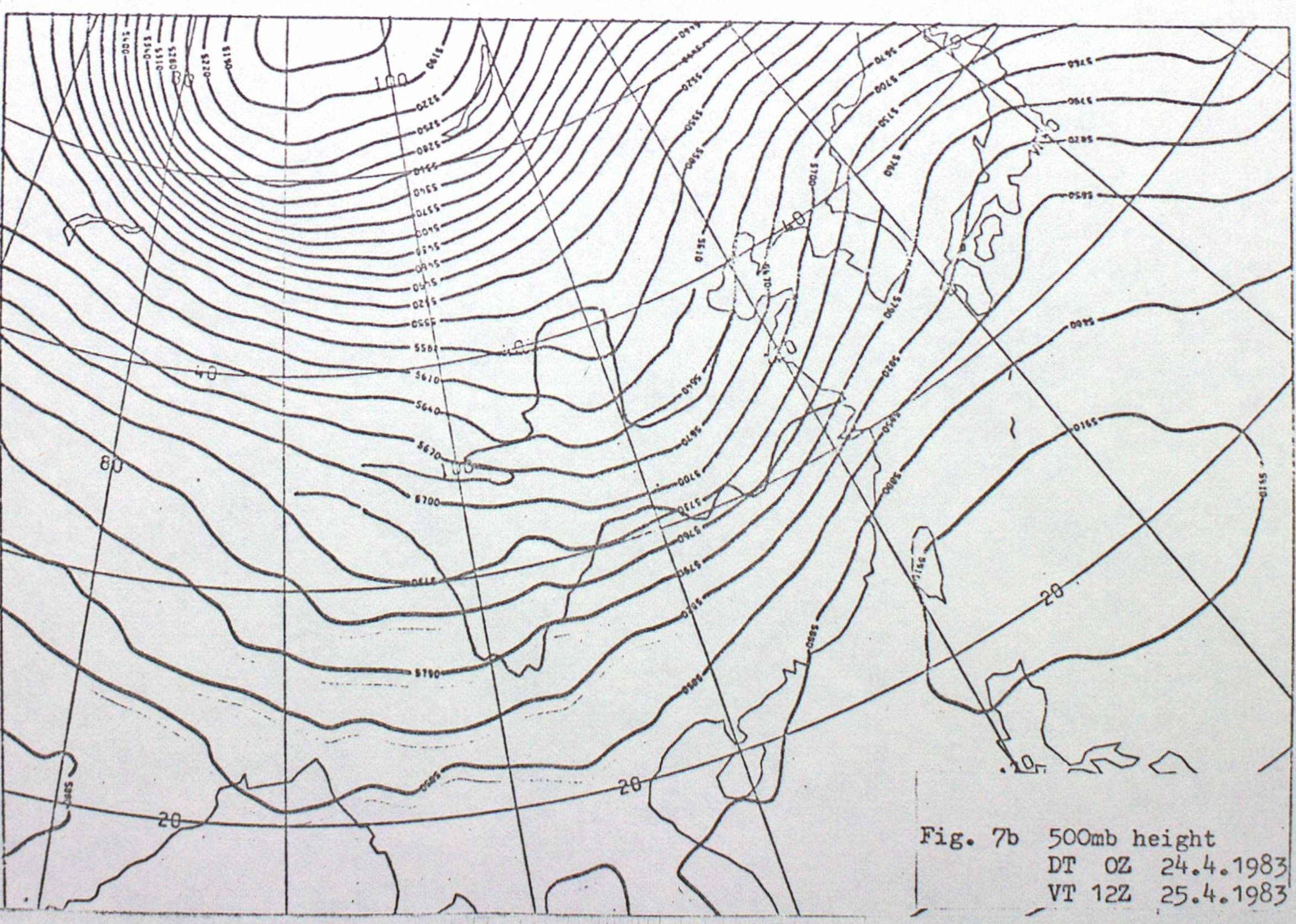

Fig. 7b 500mb height
DT 0Z 24.4.1983
VT 12Z 25.4.1983

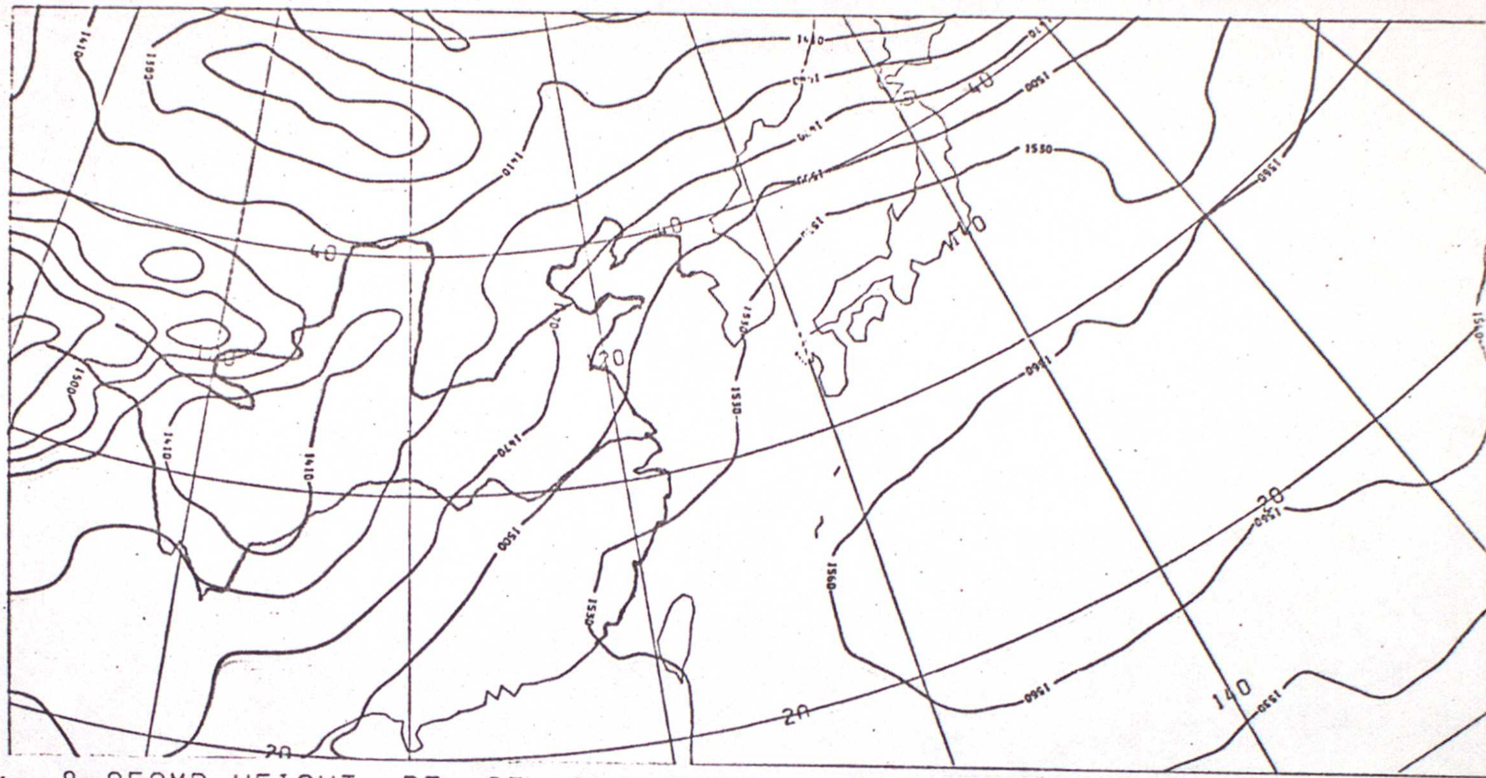

Fig. 8a 850MB HEIGHT DT 0Z 24/4/1983
VT 12Z 24/4/1983

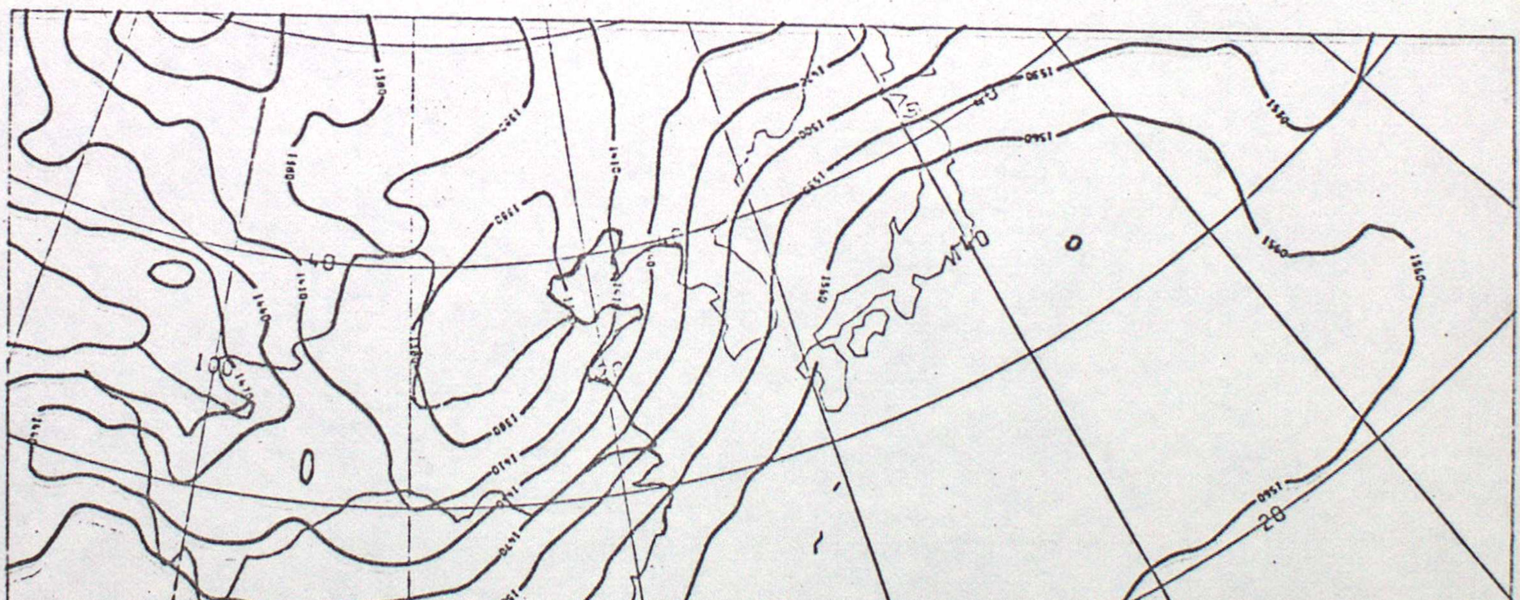

Fig. 8b 850MB HEIGHT DT 0Z 24/4/1983
VT 12Z 25/4/1983

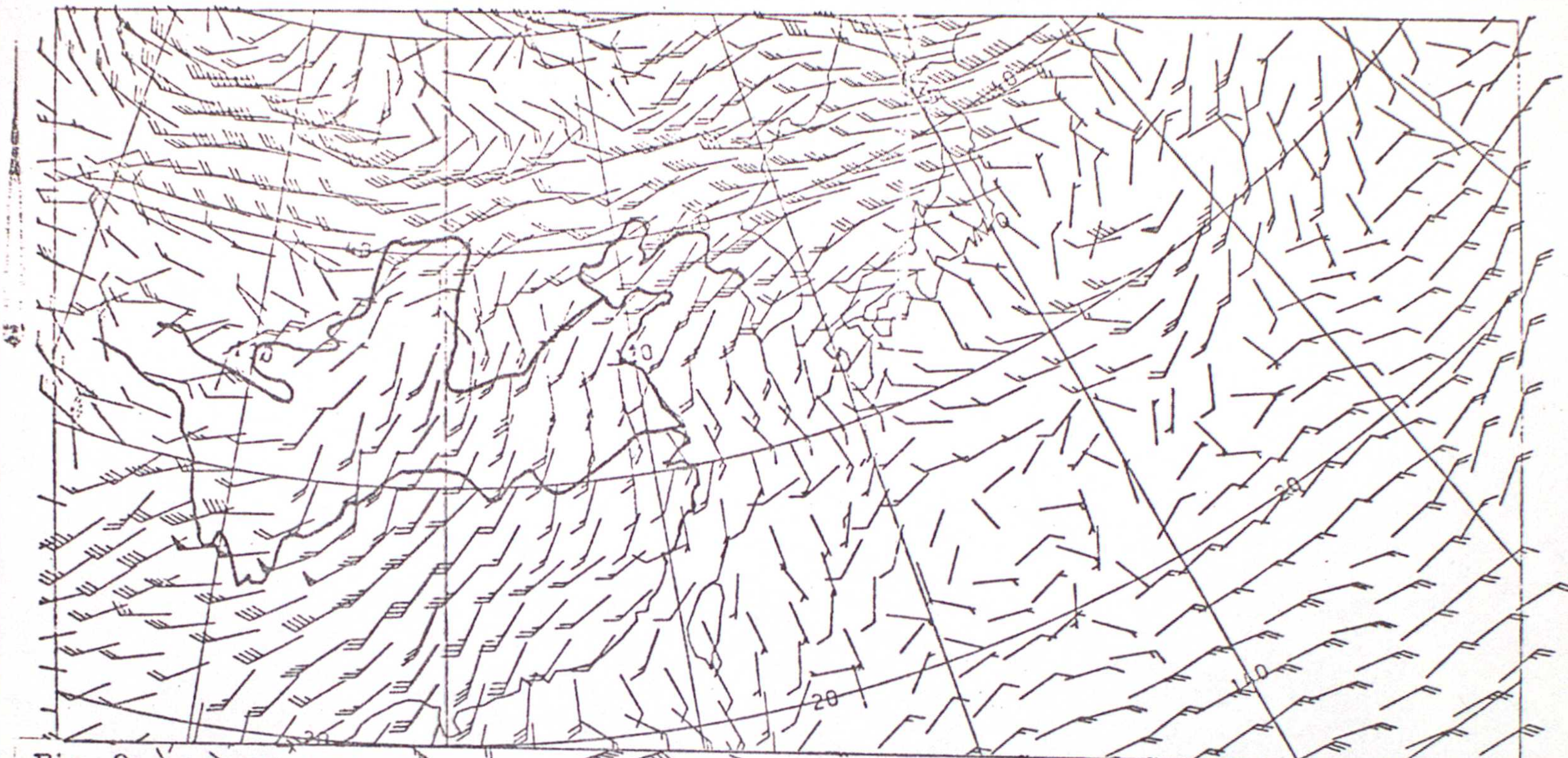

Fig. 9a WINDS (KT) AT SIGMA-LEVEL 4 DT 0Z 24/4/1983
VT 12Z 24/4/1983

Fig. 9b WINDS (KT) AT SIGMA-LEVEL 4 DT 0Z 24/4/1983
VT 12Z 25/4/1983

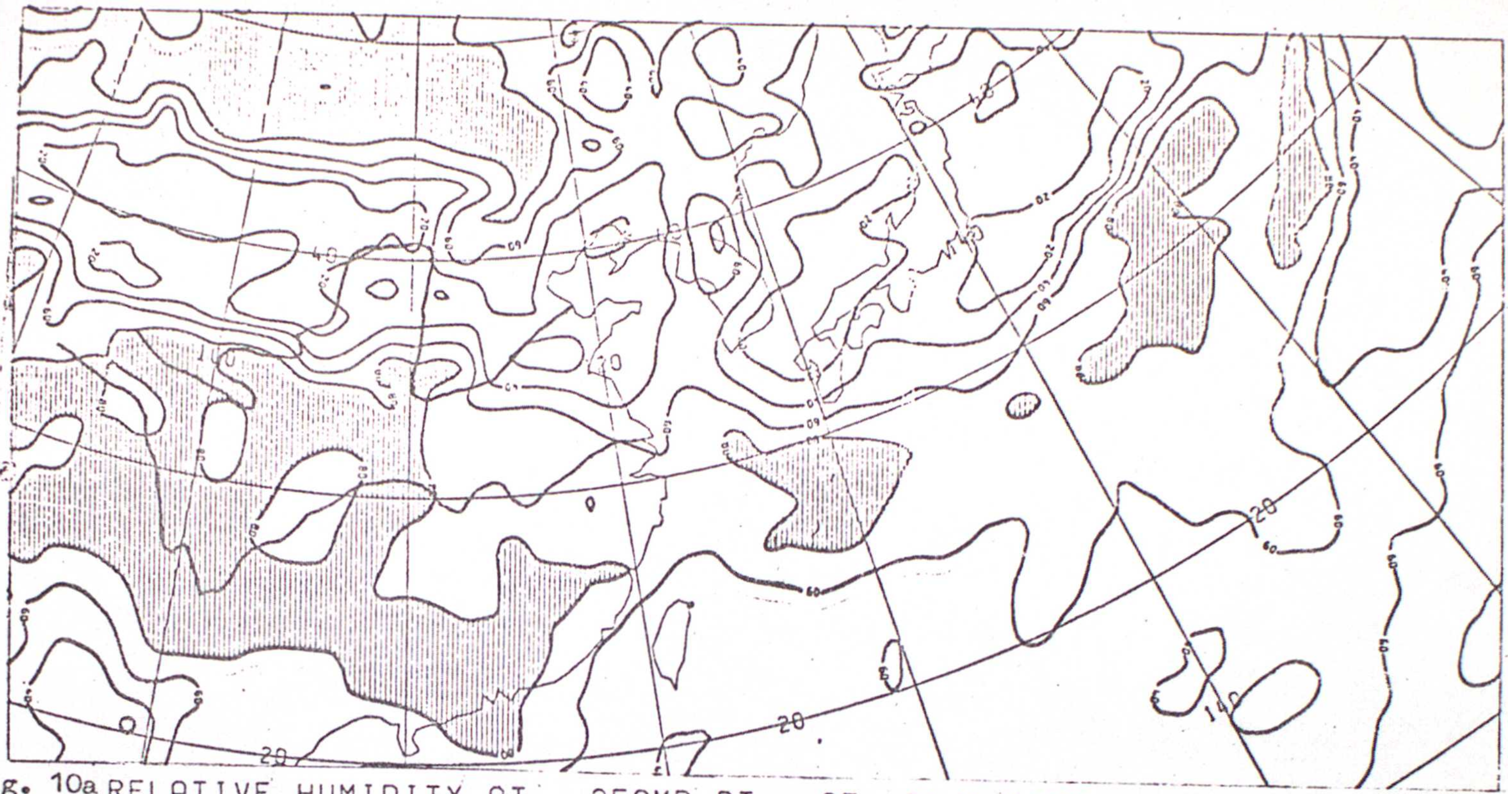

Fig. 10a RELATIVE HUMIDITY AT 850MB DT OZ 24/4/1983
VT 12Z 24/4/1983

Fig. 10b RELATIVE HUMIDITY AT 850MB DT OZ 24/4/1983
VT 12Z 25/4/1983

Fig. 11a Streamline 850mb 00 GMT 29.7.1983

Fig. 11b

WINDS (KT) AT SIGMA-LEVEL 4 DT 0Z 28/7/1983
VT 0Z 29/7/1983

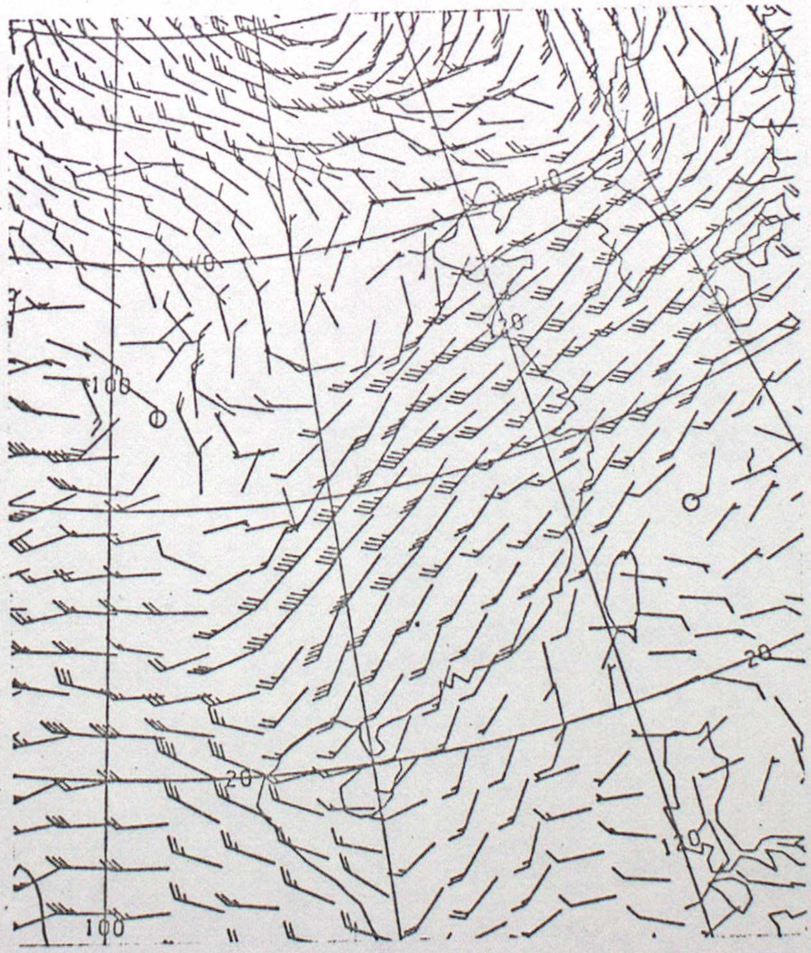

Fig. 12a RAINFALL(MM) 0000/28/07/83 TO 1200/28/07/83

Fig. 12b RAINFALL(MM) 1200/28/08/83 TO 0000/29/08/83

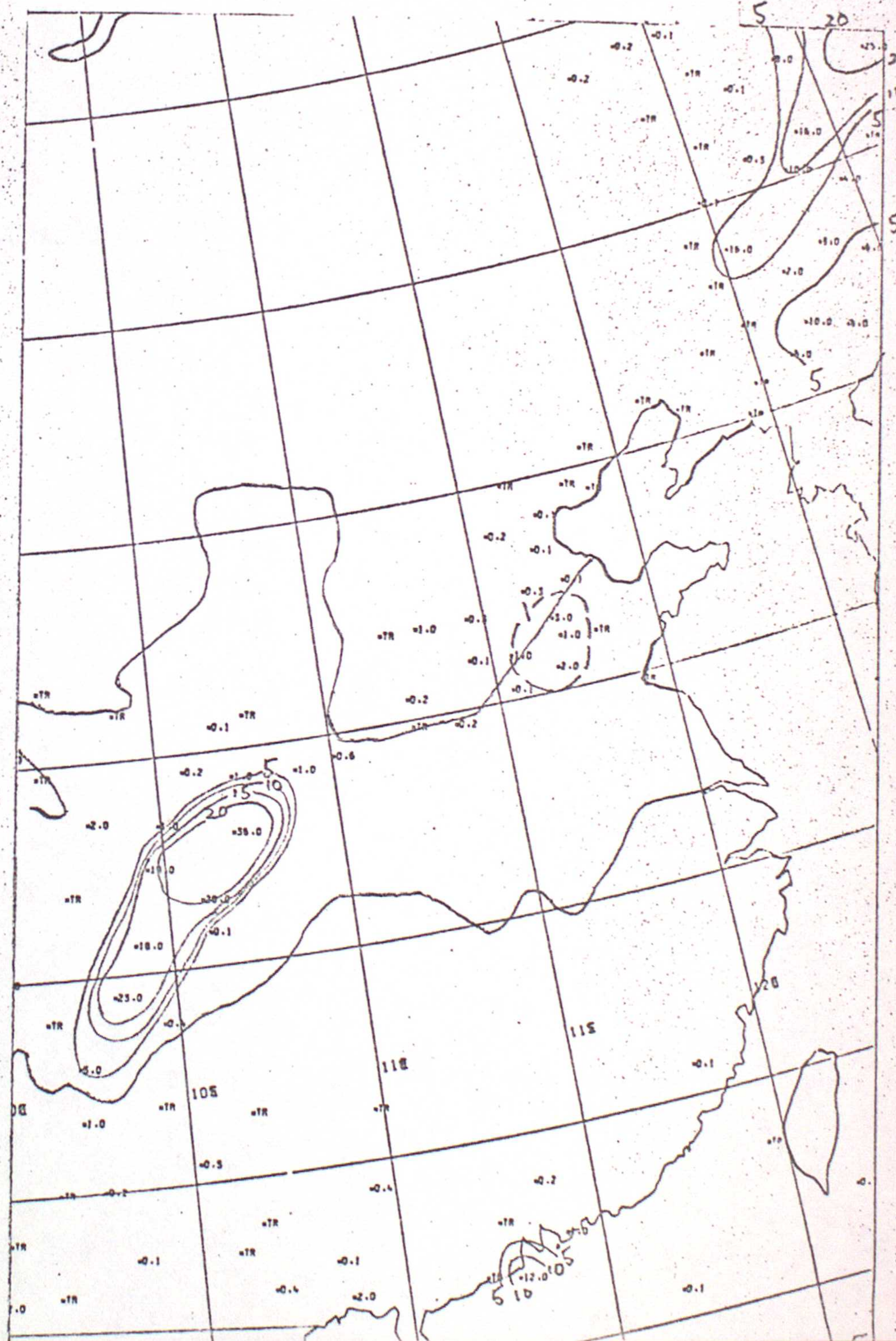

Fig. 12c RAINFALL(MM) 0000/29/07/83 TO 1200/29/07/83

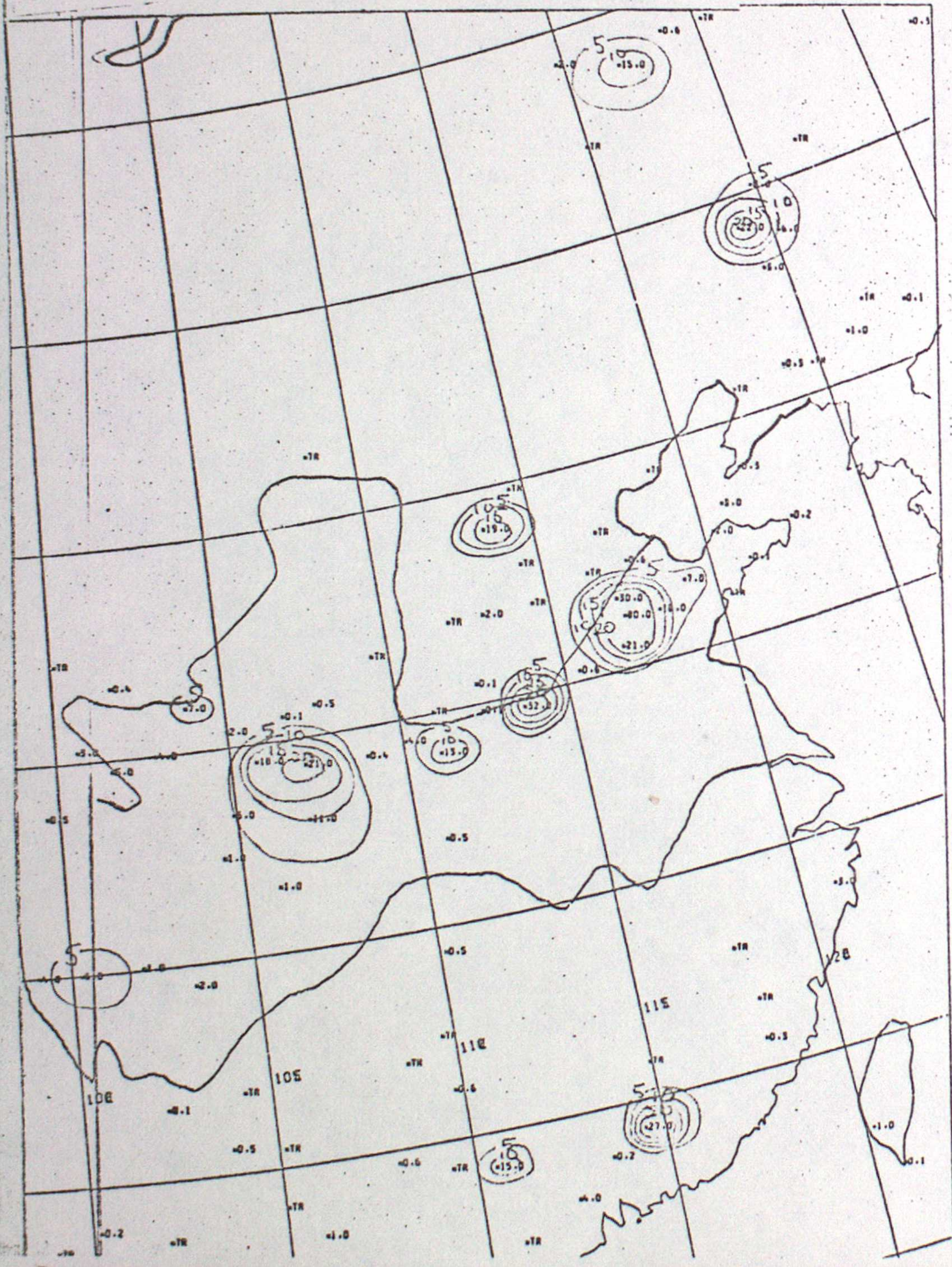

Fig. 12d RAINFALL(MM) 1200/29/07/83 TO 0000/30/07/83

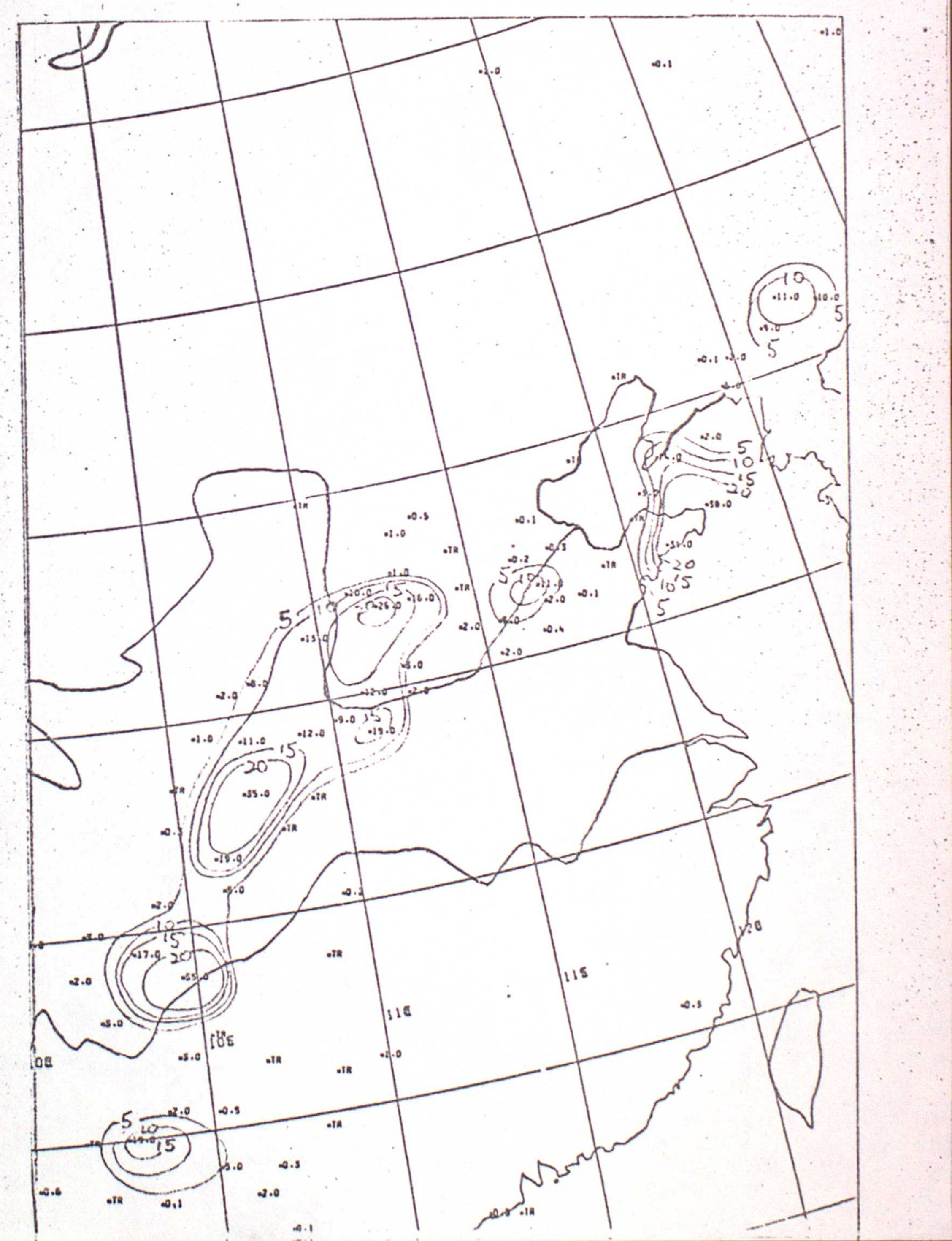

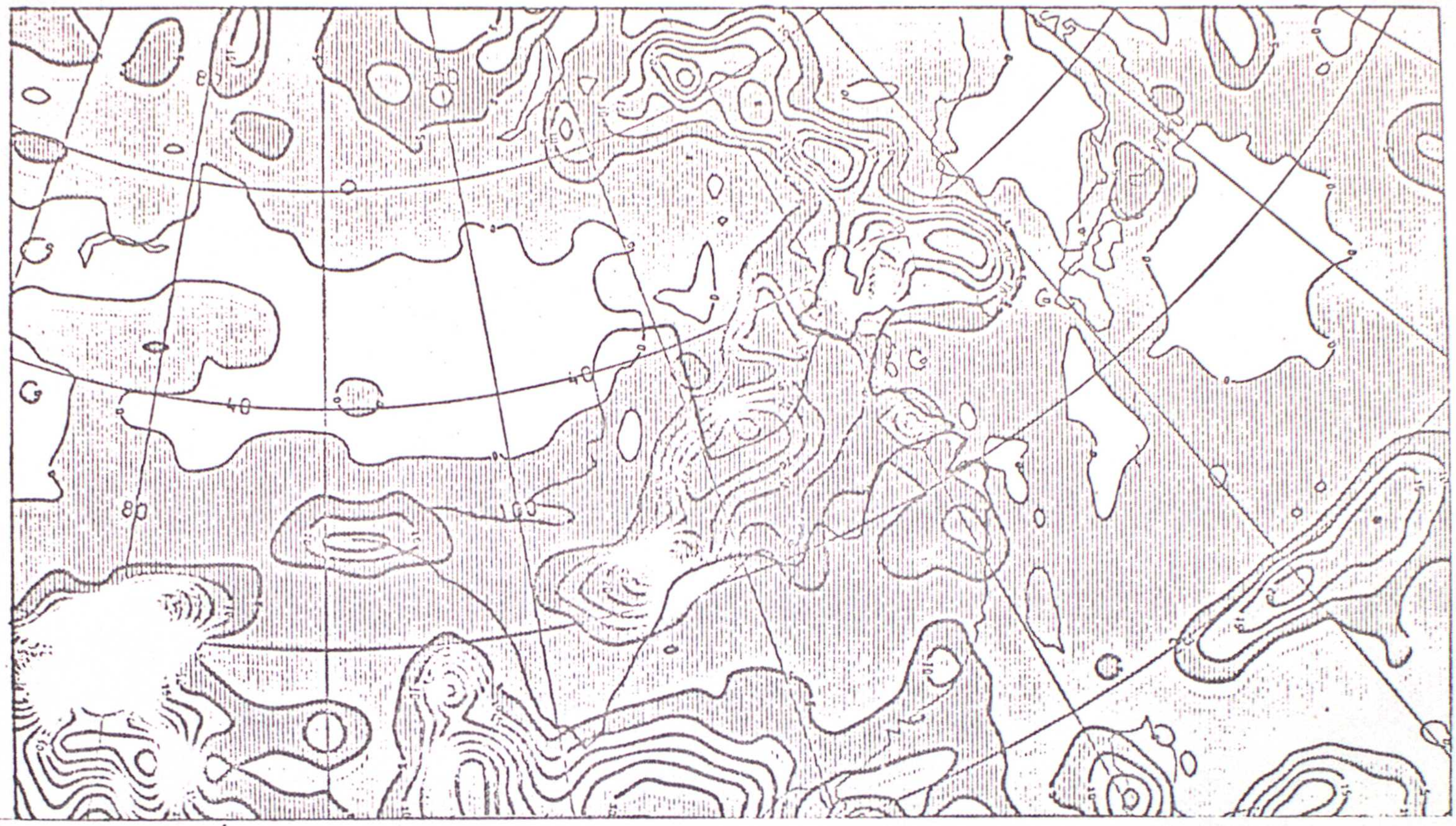

Fig. 13a TOTAL ACCUMULATED PRECIPITATION MM DT 0Z 28/7/1983
VT 12Z 28/7/1983

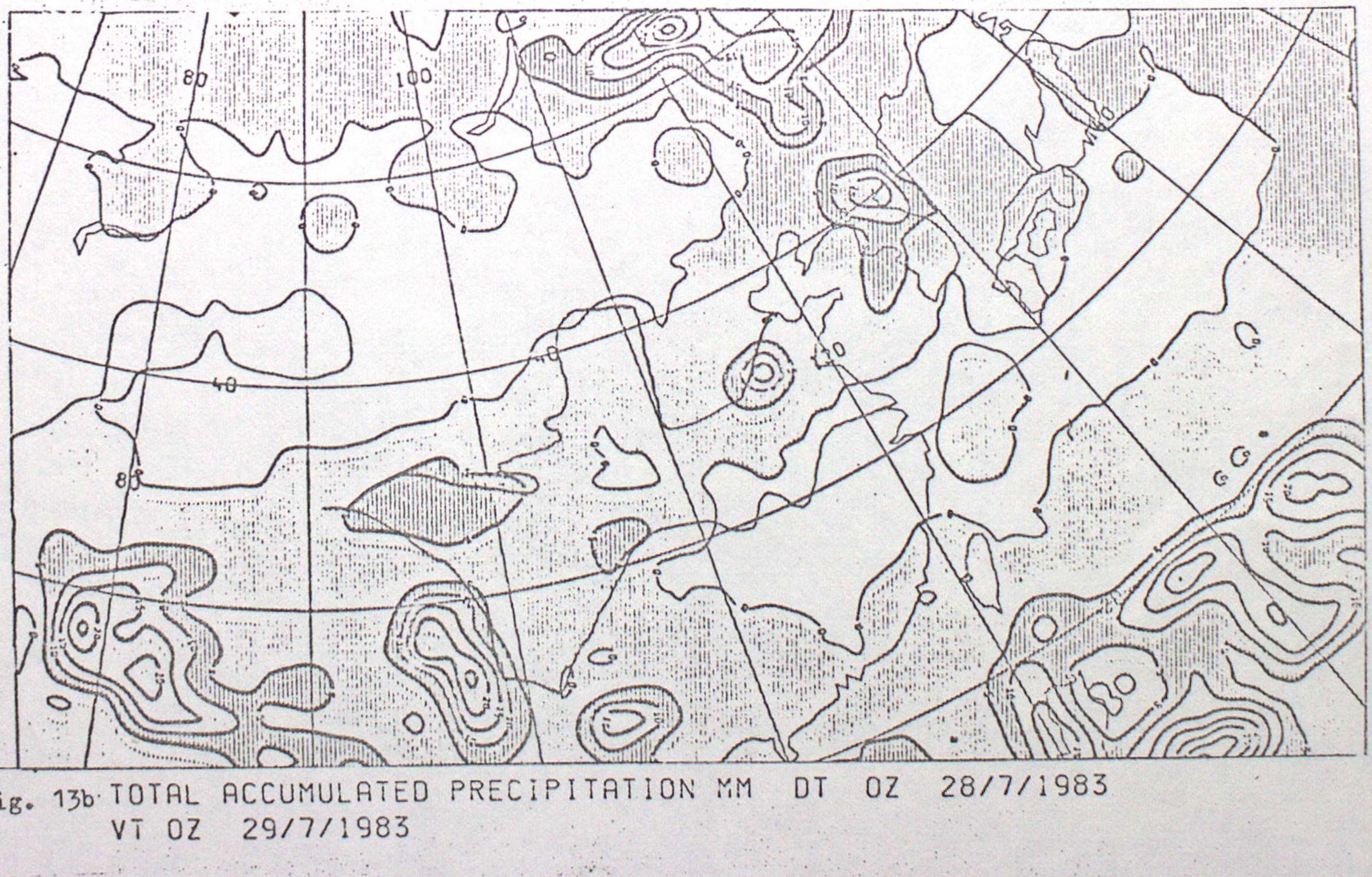

Fig. 13b TOTAL ACCUMULATED PRECIPITATION MM DT 0Z 28/7/1983
VT 0Z 29/7/1983

Fig. 13c TOTAL ACCUMULATED PRECIPITATION MM DT OZ 28/7/1983
VT 12Z 29/7/1983

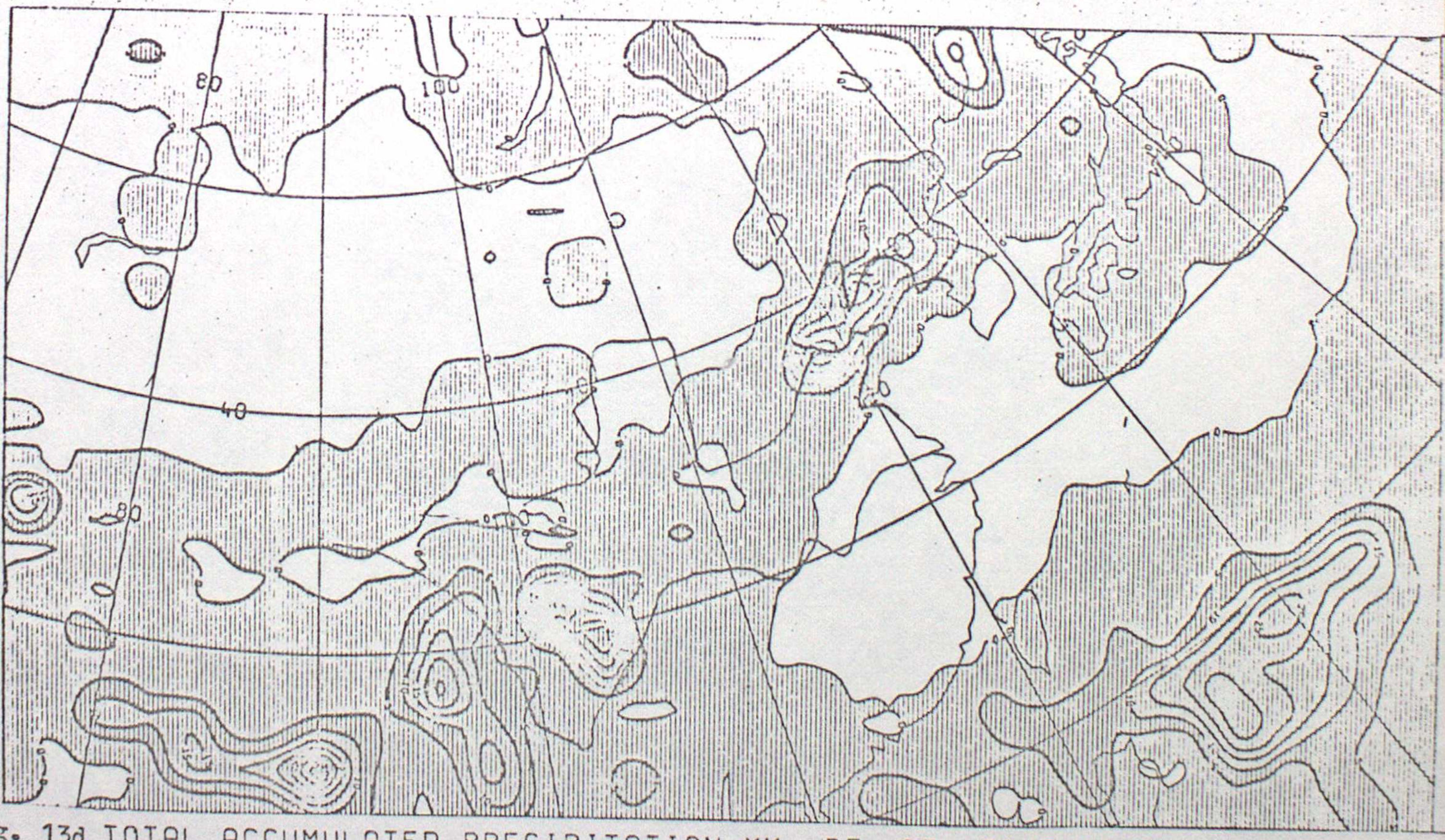

Fig. 13d TOTAL ACCUMULATED PRECIPITATION MM DT OZ 28/7/1983
VT OZ 30/7/1983

Fig. 14a Isotach (M/S) 500mb
12GMT 29.7.1983

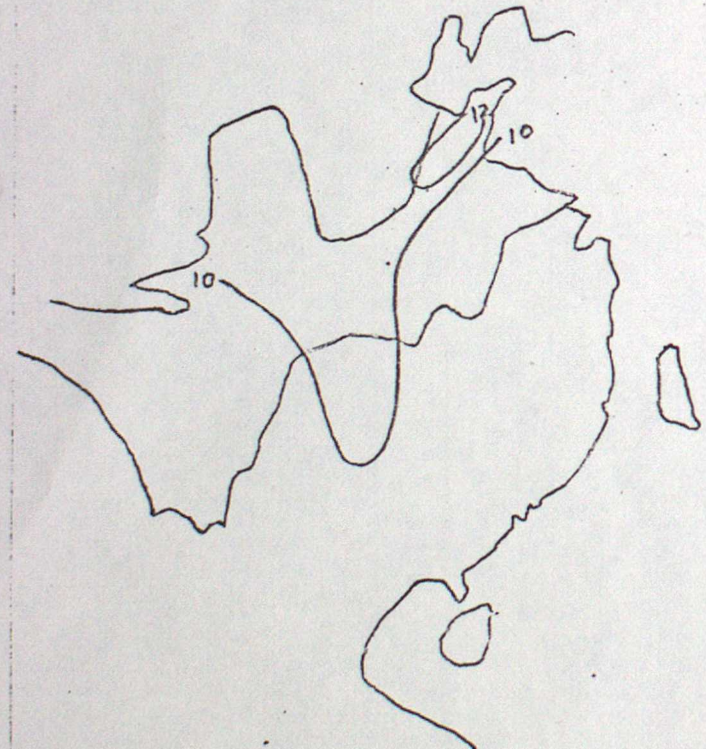

Fig. 14b The same as Fig.14a
but 700mb

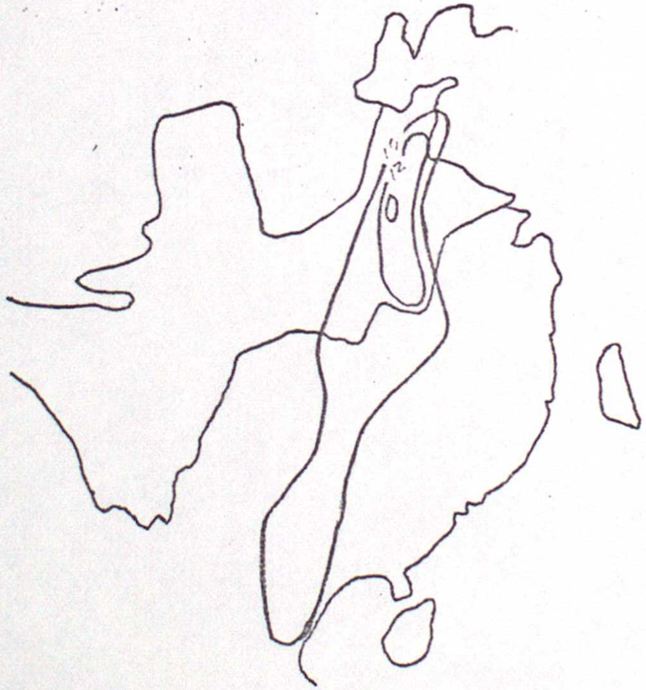

Fig. 14c The same as Fig.14a
but 850mb

Fig. 15a Isotach (M/S) sigma-level 8,
DT 0Z 28.7.1983
VT 12Z 29.7.1983

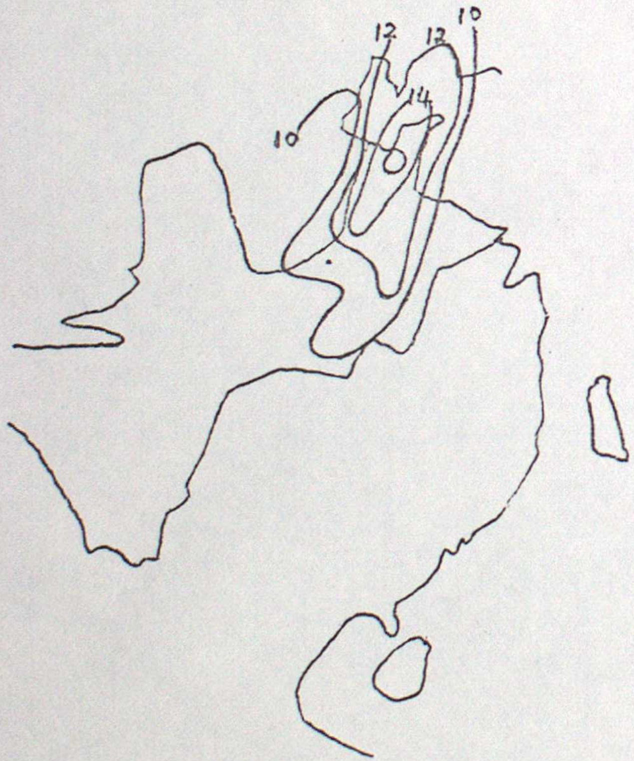

Fig. 15b The same as Fig. 15a
but sigma level 6

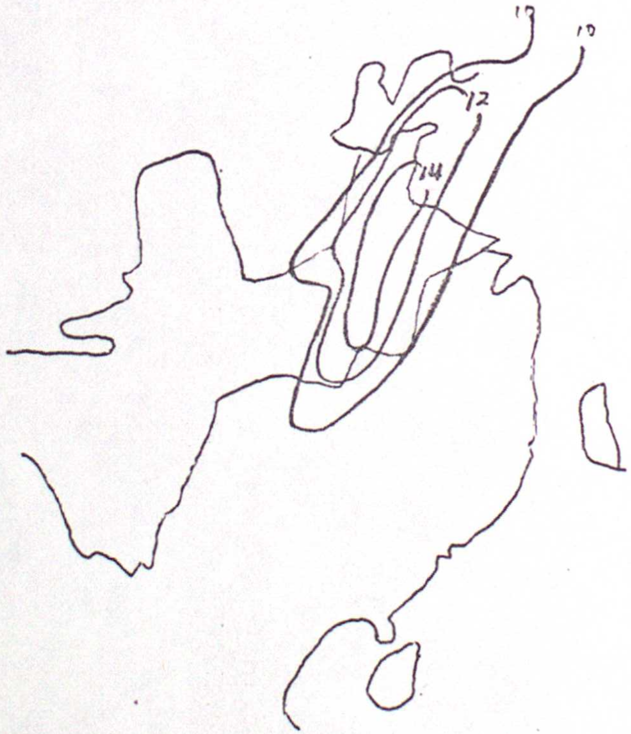

Fig. 15c The same as Fig. 15a
but sigma level 4

Fig. 16 The test area